UvA-DARE (Digital Academic Repository)

Electronic structure of the perturbed blue copper site in nitrite reductase: spectroscopic properties, bonding and implications for the entatic/rack state.

LaCroix, L.B.; Shadle, S.E.; Wang, Y.; Averill, B.A.; Hedman, B.; Hodgson, K.O.; Solomon, E.

Link to publication

Electronic Structure of the Perturbed Blue Copper Site in Nitrite Reductase: Spectroscopic Properties, Bonding, and Implications for the Entatic/Rack State

Louis B. LaCroix,[†] Susan E. Shadle,[†] Yaning Wang,[‡] Bruce A. Averill,[‡,§] Britt Hedman,[⊥] Keith O. Hodgson,[†,⊥] and Edward I. Solomon*,[†]

Contribution from the Department of Chemistry, Stanford University, Stanford, California 94305, Department of Chemistry, University of Virginia, Charlottesville, Virginia 22901, and Stanford Synchrotron Radiation Laboratory, Stanford University, Stanford, California 94309

Received April 12, 1996[⊗]

Abstract: Low-temperature optical absorption, circular dichroism, magnetic circular dichroism, and sulfur K-edge X-ray absorption spectra have been measured for the green "blue" copper center (type 1) in *Achromobacter cycloclastes* nitrite reductase. Combined with density functional calculations, the results of these spectroscopies have been used to define the extremely "perturbed" electronic structure of this site relative to that of the prototypical "classic" site found in plastocyanin. Experimentally calibrated density functional calculations have been further used to determine the specific geometric distortions which generate the perturbed electronic structure. These studies indicate that the principal electronic structure changes in nitrite reductase, relative to plastocyanin, are a rotation of the Cu $d_{x^2-y^2}$ half-filled, highest occupied molecular orbital (HOMO) and an increase in the ligand field strength at the Cu center. The HOMO rotation increases the pseudo-σ interaction and decreases the π interaction of the cysteine (Cys) sulfur with Cu $d_{x^2-y^2}$. Furthermore, significant methionine (Met) sulfur character is mixed into the HOMO due to increased overlap with Cu $d_{x^2-y^2}$. These changes in Cu−ligand interactions result in the redistribution of absorption intensity in the charge transfer and ligand field transitions. Additionally, the new S(Met)−Cu interaction accounts for the unexpectedly high sulfur covalency in the HOMO. The increase in ligand field strength shifts all the d → d transitions in nitrite reductase to ∼1000 cm^{-1} higher energy than their counterparts in plastocyanin, which accounts for the EPR spectral differences between the type 1 sites in these complexes. The geometric distortion primarily responsible for the electronic structure changes in nitrite reductase, relative to plastocyanin, is determined to involve a coupled angular movement of the Cys and Met residues toward a more flattened tetrahedral (toward square planar) structure. This movement is consistent with a tetragonal Jahn−Teller distortion resulting from the shorter Cu−S(Met) bond in nitrite reductase relative to plastocyanin. This increased Jahn−Teller distortion implies that the type 1 site is "less entatic" than that in plastocyanin.

Introduction

Blue copper sites, which are present in a number of protein environments, have been extensively studied as prototype systems for long-range electron transfer in biology.[1,2] Compared to small-molecule (*i.e.*, "normal") cupric complexes, oxidized blue copper centers exhibit several distinguishing characteristics[3−12] that reflect novel electronic structures which can make

a significant contribution to reactivity.[13,14] These include an absorption band near 600 nm, called the "blue" band, with an intensity ($\epsilon_{max} \approx 3000-6000$ M^{-1} cm^{-1}) which is 100−1000 times that of normal copper ligand field transitions. In the EPR spectra, the Cu parallel hyperfine coupling constant, $A_{\parallel}$, is reduced by a factor of 2 or more from $(130-180) \times 10^{-4}$ cm^{-1} in normal centers to $<80 \times 10^{-4}$ cm^{-1} in blue centers. Blue copper proteins often have high reduction potentials (+184 to +800 mV) relative to that of the aqueous Cu(II)/Cu(I) couple (+160 mV).

While all blue copper sites differ from normal copper complexes as described above, variations within this class of proteins also exist.[2,14−17] In addition to the intense absorption peak at ∼600 nm, blue copper proteins also exhibit weaker absorption of variable intensity at ∼450 nm. Furthermore, the

(1) Adman, E. T. In *Advances in Protein Chemistry*; Anfinsen, C. B., Richards, F. M., Edsall, J. T., Eisenberg, D. S., Eds.; Academic Press, Inc.: San Diego, 1991; Vol. 42, pp 145−198.
(2) Adman, E. T. In *Topics in Molecular and Structural Biology: Metalloproteins*; Harrison, P., Ed.; MacMillan: New York, 1985; Vol. 1, pp 1−42.
(3) Blumberg, W. E.; Peisach, J. *Biochim. Biophys. Acta* **1966**, *126*, 269−273.
(4) Brill, A. S.; Bryce, G. F. *J. Chem. Phys.* **1968**, *48*, 4398−4404.
(5) Fee, J. A. *Struct. Bonding (Berlin)* **1975**, *23*, 1−60.
(6) Gray, H. B.; Solomon, E. I. In *Copper Proteins*; Spiro, T. G., Ed.; Wiley: New York, 1981; pp 1−39.
(7) Solomon, E. I. In *Copper Coordination Chemistry: Biochemical & Inorganic Perspectives*; Karlin, K., Zubieta, J., Eds.; Adenine Press: Guilderland, NY, 1982; pp 1−22.
(8) Solomon, E. I.; Penfield, K. W.; Wilcox, D. E. *Struct. Bonding (Berlin)* **1983**, *53*, 1−57.
(9) Dorfman, J. R.; Bereman, R. D.; Whango, M.-H. In *Copper Coordination Chemistry: Biochemical and Inorganic Perspectives*; Karlin, K., Zubieta, J., Eds.; Adenine Press: Guilderland, NY, 1982; pp 75−96.
(10) Blair, D. F.; Campbell, G. W.; Schoonover, J. R.; Chan, S. I.; Gray, H. B.; Malmstrom, B. G.; Pecht, I.; Swanson, B. I.; Woodruff, W. H.; Cho, W. K.; English, A. M.; Fry, H. A.; Lum, V.; Norton, K. A. *J. Am. Chem. Soc.* **1985**, *107*, 5755−5766.
(11) Roberts, J. E.; Cline, J. F.; Lum, V.; Freeman, H. C.; Gray, H. B.; Peisach, J.; Reinhammer, B.; Hoffman, B. M. *J. Am. Chem. Soc.* **1984**, *106*, 5324−5330.
(12) Scott, R. A.; Hahn, J. E.; Doniach, S.; Freeman, H. C.; Hodgson, K. O. *J. Am. Chem. Soc.* **1982**, *104*, 5364−5369.
(13) Solomon, E. I.; Lowery, M. D. *Science* **1993**, *259*, 1575−1581.
(14) Solomon, E. I.; Baldwin, M. J.; Lowery, M. D. *Chem. Rev.* **1992**, *92*, 521−542.

$g_\perp$ region in the EPR spectrum of blue copper proteins show various degrees of rhombic distortion and copper hyperfine coupling in the g_x region. The better understood "classic" blue copper proteins, such as plastocyanin and azurin, shows very little absorption in the 450 nm region and display axial ($g_x \approx g_y$) EPR signals with small hyperfine splittings in the $g_\perp$ region. In contrast, "perturbed" blue copper sites, like those in stellacyanin and pseudoazurin, exhibit rhombic EPR signals, relatively large A_x values, and increased 450 nm absorption intensity relative to those in classic blue copper proteins. Nitrite reductase (NiR) from *Achromobacter cycloclastes* is an ideal system for study of the limiting case of a strongly perturbed site.[18,19] This enzyme, which is involved in the denitrification pathway of anaerobic bacteria,[20,21] accepts electrons from pseudoazurin at a blue site (called type 1) and reduces NO_2^- to NO at a second, normal Cu (type 2).[22,23] Despite having the same ligand set as that of plastocyanin (Pc) (*vide infra*),[24] the EPR spectrum of the type 1 center in nitrite reductase exhibits all the features associated with perturbed sites detailed above, and the absorption spectrum is extremely perturbed. The ∼600 nm absorption envelope is reduced in intensity by a factor of ∼3 relative to classic sites while the ∼450 nm absorption increases so dramatically that it is more intense than the 600 nm blue band, resulting in the green color of the enzyme.[18,19] Additionally, another transition envelope is observed at ∼385 nm, which is not present in the spectra of classic and most other perturbed sites.

High-resolution X-ray crystallographic studies of poplar plastocyanin (*Populus nigra*) by Freeman *et al.*[25] have indicated that the copper coordination sphere in blue sites is a distorted tetrahedron (Figure 1B) which consists of two typical imidazole $N_{\delta 1}$–Cu bonds (1.92 and 2.04 Å) from histidine (His) residues, a short cysteine (Cys) thiolate S_γ–Cu bond (2.07 Å), and a long methionine (Met) thioether S_δ–Cu bond (2.82 Å). The Cu ion lies slightly (0.36 Å) out of the NNS plane formed by the strong, equatorial His and Cys ligands. Crystal structures for other blue copper containing proteins indicate that the active site structures in these systems are very similar and that ligation and geometry are highly conserved in blue copper centers.[24,26-33] The crystal structure of nitrite reductase reveals, however, that subtle
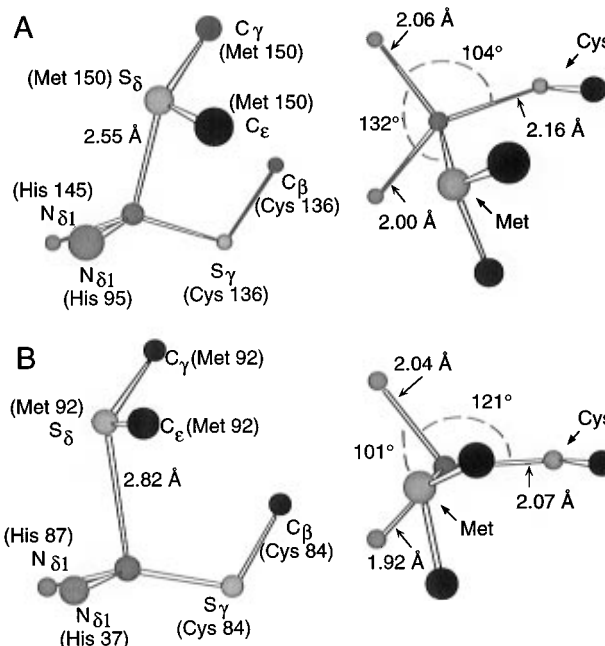
Figure 1. Structure of the oxidized blue copper centers in *A. cycloclastes* nitrite reductase[24] (A) and poplar plastocyanin[25] (B) viewed with the cysteine−histidine−histidine (Cys−His−His) NNS plane perpendicular (left) and parallel (right) to the plane of the paper. Compared with plastocyanin, bonds to the residues in the equatorial plane in nitrite reductase expand while the axial methionine S(Met)−Cu bond contracts, and the Cu ion is pulled farther out of the NNS plane toward S(Met). The angular differences in the orientation of the ligands in nitrite reductase relative to plastocyanin are most apparent in the parallel view, in which the Met ligand is seen to tilt toward the NNS plane and the Cu−S(Cys) bond is rotated with respect to the His nitrogens.

geometric differences exist.[24] The bonds to the equatorial ligands of the type 1 site in oxidized nitrite reductase expand relative to those in plastocyanin (Figure 1A), with 2.17 Å Cu−S(Cys) and 2.06 and 2.00 Å Cu−N(His) bond lengths, while the axial Cu−S(Met) bond contracts to 2.55 Å.[34] Furthermore, the Cu ion is raised farther out of the equatorial NNS plane (0.54 Å), and angular changes at the site, particularly with respect to the Cys and Met ligation, are evident (Figure 1A). It should be noted that the enzyme is a trimer, with one type 1 and one type 2 copper per monomer. The type 2 Cu site, which is required for enzymatic activity and is connected *via* a 12.5 Å His−Cys pathway to the type 1 site through which electron transfer likely occurs, can be selectively removed to form inactive type 2 depleted (T2D) nitrite reductase.[35]

Investigations of the electronic structure of the classic site in plastocyanin have shown that the distinctive spectral features of the oxidized site arise from the ligand set and geometry.[13,14] EPR data have indicated that the half-occupied redox-active orbital (highest occupied molecular orbital (HOMO)) is Cu $3d_{x^2-y^2}$ and the g_z vector of the site is oriented 5° away from

(15) Lu, Y.; LaCroix, L. B.; Lowery, M. D.; Solomon, E. I.; Bender, C. J.; Peisach, J.; Roe, J. A.; Gralla, E. B.; Valentine, J. S. *J. Am. Chem. Soc.* **1993**, *115*, 5907−5918.

(16) Gewirth, A. A.; Cohen, S. L.; Schugar, H. J.; Solomon, E. I. *Inorg. Chem.* **1987**, *26*, 1133−1146.

(17) Andrew, C. R.; Yeom, H.; Valentine, J. S.; Karlsson, B. G.; Bonander, N.; van Pouderoyen, G.; Canters, G. W.; Loehr, T. M.; Sanders-Loehr, J. *J. Am. Chem. Soc.* **1994**, *116*, 11489−11498.

(18) Iwasaki, H.; Noji, S.; Shidara, S. *J. Biochem.* **1975**, *78*, 355−361.

(19) Liu, M.-Y.; Liu, M.-C.; Payne, W. J.; LeGall, J. *J. Bacteriol.* **1986**, *166*, 604−608.

(20) Berks, B. C.; Ferguson, S. J.; Moir, J. W. B.; Richardson, D. J. *Biochim. Biophys. Acta* **1995**, *1232*, 97−173.

(21) Ye, R. W.; Averill, B. A.; Tiedje, J. M. *Appl. Environ. Microbiol.* **1994**, *60*, 1053−1058.

(22) Hulse, C. L.; Tiedje, J. M.; Averill, B. A. *Anal. Biochem.* **1988**, *172*, 420−426.

(23) Godden, J. W.; Turley, S.; Teller, D. C.; Adman, E. T.; Liu, M. Y.; Payne, W. J.; Legall, J. *Science* **1991**, *253*, 438−442.

(24) Adman, E. T.; Godden, J. W.; Turley, S. *J. Biol. Chem.* **1995**, *270*, 27458−27474.

(25) Guss, J. M.; Bartunik, H. D.; Freeman, H. C. *Acta Crystallogr.* **1992**, *B48*, 790−811.

(26) Collyer, C. A.; Guss, J. M.; Sugimura, Y.; Yoshizuka, F.; Freeman, H. C. *J. Mol. Biol.* **1990**, *211*, 617−632.

(27) Baker, E. N. *J. Mol. Biol.* **1988**, *203*, 1071−1095.

(28) Shepard, W. E. B.; Anderson, B. F.; Lewandoski, D. A.; Norris, G. E.; Baker, E. N. *J. Am. Chem. Soc.* **1990**, *112*, 7817−7819.

(29) Nar, H.; Messerschmidt, A.; Huber, R.; van de Kamp, M.; Canters, G. W. *J. Mol. Biol.* **1991**, *221*, 765−772.

(30) Zhu, D. W.; Dahms, T.; Willis, K.; Szabo, A. G.; Lee, X. *Arch. Biochem. Biophys.* **1994**, *308*, 469−470.

(31) Coyle, C. L.; Zumft, W. G.; Kroneck, P. M. H.; Korner, H.; Jakob, W. *Eur. J. Biochem.* **1985**, *153*, 459−467.

(32) Jin, H.; Thomann, H.; Coyle, C. L.; Zumft, W. G. *J. Am. Chem. Soc.* **1989**, *111*, 4262−4269.

(33) Messerschmidt, A.; Ladenstein, R.; Huber, R.; Bolognesi, M.; Avigliano, L.; Petruzzelli, R.; Rossi, A.; Finazzi-Agro, A. *J. Mol. Biol.* **1992**, *224*, 179−205.

(34) At the resolutions of the crystal structures (1.3 and 1.7 Å for plastocyanin and nitrite reductase, respectively) the estimated standard deviations for the bond lengths are 0.04 and 0.03 Å for nitrite reductase and plastocyanin, respectively. With this degree of precision, the 0.1 Å difference in Cu−S(Cys) bond lengths of the two sites may not be statistically significant; however, resonance Raman frequencies, total charge transfer intensities, and other spectroscopic data strongly indicate that these bonds differ appreciably in length (*vide infra*).

(35) Libby, E.; Averill, B. A. *Biochem. Biophys. Res. Commun.* **1992**, *187*, 1529−1535.

the Cu−S(Met) bond, which results in the Cu $3d_{x^2-y^2}$ orbital lying within 15° of the NNS(Cys) equatorial plane.[36−38] This orbital exhibits a large and highly anisotropic degree of covalency. X-ray absorption spectroscopy (XAS) at the S K-edge[39] and Cu L-edge[40] has indicated that the HOMO contains 38% S(Cys) character and only ∼40% Cu character, and electronic structure calculations[41] indicate that only ∼4% N(His) character is present in the HOMO (because the Cu−S(Met) bond is oriented approximately perpendicular to the HOMO, no S(Met) character is present in the HOMO). The small EPR hyperfine splitting in blue copper centers has been shown to originate from this extremely high covalency.[39,42] Polarized XAS of the pre-edge transition at the Cu K-edge of plastocyanin single crystals[12] has been further used[39] to establish that an alternate mechanism for reduction in the EPR hyperfine splitting, geometrically derived Cu $4p_z$ mixing into the HOMO,[43−45] is not operative. Low-temperature optical spectra (polarized single-crystal absorption, circular dichroism (CD), and magnetic circular dichroism (MCD)) coupled with self-consistent field-Xα-scattered wave (SCF-Xα-SW) molecular orbital calculations, calibrated to experimental g values, have been used to assign the ligand field and charge transfer transitions in plastocyanin.[41] The charge transfer spectrum was found to be inverted from the low-energy, weak π/high-energy, intense σ charge transfer transition pattern typically found in normal copper complexes. The intense 600 nm blue band was assigned to the S(Cys) pπ → Cu $3d_{x^2-y^2}$ transition, with the weaker S(Cys) pσ → Cu $3d_{x^2-y^2}$ charge transfer transition occurring at higher energy. It should be noted that the C−S−Cu bond angle of 112° splits the π set of orbitals in free cysteine into "π" and "pseudo-σ" orbitals in the protein.[42] The HOMO orientation was determined to be responsible for the unusual optical spectral features. The strong π S(Cys)−Cu interaction orients the $d_{x^2-y^2}$ orbital so that the Cu−S(Cys) bond bisects the lobes of the orbital. This anisotropic covalency has been shown to have mechanistic significance as it provides an efficient superexchange pathway for electron transfer through the cysteine residue.[13,14,46]

The geometric structure of the reduced blue copper site in plastocyanin is remarkably similar to that of the oxidized site.[47] The absence of a distortion toward a tetragonal geometry upon oxidation of the reduced active site had been ascribed to an "entatic"[48] or "rack"[49−51] state, in which the protein environment mismatches the lowest energy conformation of Cu(II), effectively imposing the reduced site geometry on the oxidized

site. The presence of Cu(II) in the Cu(I)-preferred pseudotetrahedral geometry, along with the presence of soft thiolate and methionine sulfur ligation, have also been used to explain the high redox potential of blue copper sites.[52−54] The nature of the bonding in the reduced d^{10} site and changes in bonding upon oxidation in plastocyanin have been defined through the use of variable-energy photoelectron spectroscopy on Cu(I) surface complexes with blue copper relevant ligands coupled with SCF-Xα-SW calculations.[55] The bonding in the reduced blue copper site was found to be dominated by donor interaction of ligands into the unoccupied 4p orbitals on Cu(I). The dominant change in the electronic structure upon oxidation involves the hole created in the $d_{x^2-y^2}$ orbital as described above. Creation of this hole leads to geometry changes consistent with those observed from X-ray studies; therefore, the reduced geometry is not imposed on the oxidized site. The feature which is imposed on the site by the protein and can be ascribed to an entatic or rack state is the long Cu−S(Met) bond, which reduces the S(Met) donor interaction with the metal. This leads to the high reduction potential, the short Cu−S(Cys) bond (which compensates for the long thioether bond), and therefore the efficient superexchange pathway and the lack of a Jahn−Teller distorting force in the oxidized site (*i.e.*, all the orbitals are greatly split in energy (*vide infra*)), which results in little geometric change on redox and hence rapid electron transfer.

The insight into the electronic and geometric structure achieved for classic blue copper active sites can now be extended to perturbed centers. In the present study, the electronic structure of the active site in nitrite reductase is defined relative to the classic blue copper site in plastocyanin in order to describe the differences in bonding associated with the spectral changes, electronic effects on the geometry of the site, and possible implications for the reactivity of blue copper sites. S K-edge XAS pre-edge intensities are used to quantitate the sulfur covalency in the HOMO relative to plastocyanin. The energies and intensities of the excited state spectral features are obtained from low-temperature absorption, CD, and MCD spectroscopies, and the different selection rules of these techniques are exploited to assign the excited state transitions. SCF-Xα-SW and linear combination of atomic orbital (LCAO) density functional electronic structure calculations are used to further probe the ground and excited state properties of the perturbed type 1 site in nitrite reductase. In conjunction with experiment, these calculations generate a detailed description of the bonding in the perturbed type 1 site in nitrite reductase relative to classic sites and its contributions to the properties of the site. The specific geometric origins of the perturbed electronic structure are determined from density functional calculations performed on a series of model sites which systematically transform the classic site in plastocyanin to the perturbed site in nitrite reductase. The effect of the electronic and geometric structure distortions in nitrite reductase relative to plastocyanin on the reactivity of these sites is addressed. Finally, the nature of the entatic or rack state in blue copper sites is further explored by examining its possible role in generating the perturbed geometric and electronic structure in nitrite reductase relative to plastocyanin.

Experimental Section

Samples. Na$_2$S$_2$O$_3$·5H$_2$O was purchased from J.T. Baker and used without further purification. Plastocyanin was isolated from spinach

(36) Penfield, K. W.; Gay, R. R.; Himmelwright, R. S.; Eickman, N. C.; Norris, V. A.; Freeman, H. C.; Solomon, E. I. *J. Am. Chem. Soc.* **1981**, *103*, 4382−4388.

(37) Solomon, E. I.; Hare, J. W.; Dooley, D. M.; Dawson, J. H.; Stephens, P. J.; Gray, H. B. *J. Am. Chem. Soc.* **1980**, *102*, 168−178.

(38) Solomon, E. I.; Hare, J. W.; Gray, H. B. *Proc. Natl. Acad. Sci. U.S.A.* **1976**, *73*, 1389−1393.

(39) Shadle, S. E.; Penner-Hahn, J. E.; Schugar, H. J.; Hedman, B.; Hodgson, K. O.; Solomon, E. I. *J. Am. Chem. Soc.* **1993**, *115*, 767−776.

(40) George, S. J.; Lowery, M. D.; Solomon, E. I.; Cramer, S. P. *J. Am. Chem. Soc.* **1993**, *115*, 2968−2969.

(41) Gewirth, A. A.; Solomon, E. I. *J. Am. Chem. Soc.* **1988**, *110*, 3811−3819.

(42) Penfield, K. W.; Gewirth, A. A.; Solomon, E. I. *J. Am. Chem. Soc.* **1985**, *107*, 4519−4529.

(43) Bates, C. A.; Moore, W. S.; Standley, K. J.; Stevens, K. W. H. *Proc. Phys. Soc.* **1962**, *79*, 73.

(44) Sharnoff, M. *J. Chem. Phys.* **1965**, *42*, 3383−3395.

(45) Roberts, J. E.; Brown, T. G.; Hoffman, B. M.; Peisach, J. *J. Chem. Soc.* **1980**, *102*, 825−829.

(46) Lowery, M. D.; Guckert, J. A.; Gebhard, M. S.; Solomon, E. I. *J. Am. Chem. Soc.* **1993**, *115*, 3012−3013.

(47) Guss, J. M.; Freeman, H. C. *J. Mol. Biol.* **1986**, *192*, 361−381.

(48) Williams, R. J. P. *Eur. J. Biochem.* **1995**, *234*, 363−381.

(49) Malmström, B. G. *Eur. J. Biochem.* **1994**, *223*, 711−718.

(50) Gray, H. B.; Malmström, B. G. *Comments Inorg. Chem.* **1983**, *II*, 203−209.

(51) Lumry, R.; Eyring, H. *J. Phys. Chem.* **1954**, *58*, 110−120.

(52) Zanello, P. *Comments Inorg. Chem.* **1988**, *8*, 45−78.

(53) Karlin, K. D.; Yandell, J. K. *Inorg. Chem.* **1984**, *23*, 1184−1188.

(54) Sakaguchi, U.; Addison, A. W. *J. Chem. Soc., Dalton Trans.* **1979**, 600−608.

(55) Guckert, J. A.; Lowery, M. D.; Solomon, E. I. *J. Am. Chem. Soc.* **1995**, *117*, 2817−2844.

chloroplasts according to published methods.[56] Native and type 2 depleted forms of nitrite reductase from *A. cycloclastes* were prepared as described previously.[35] The type 1 sites in all samples of native and T2D nitrite reductase were fully loaded (3.0 Cu per trimer). Type 2 sites were partially occupied, with the native samples containing 2.4−2.6 Cu per trimer and the T2D samples containing 0.4−0.5 Cu per trimer. Specific activities, measured at room temperature using the horse heart cytochrome *c* method,[22] ranged from 21.5 to 21.7 U/mg for native and 3.3−8.1 U/mg for T2D nitrite reductase samples. The observed type 1 spectral features were identical in both native and T2D samples.

Sulfur K-Edges. A. Sample Preparation. Nitrite reductase sulfur K-edge measurements were made at ∼4 °C. The sample temperature was controlled with a cryostat which utilized liquid nitrogen cooled gases. During measurement, the sample space was purged with cold He gas. The protein solution (0.51 mM in 100 mM Tris−HCl, pH 7.0) was preequilibrated in a buffer-saturated He atmosphere for ∼1 h to minimize bubble formation in the sample cell. The protein solution was loaded *via* syringe into an Al block sample holder sealed in front by a 6.35 μm thick polypropylene window. UV−vis spectroscopy was used to verify the integrity of the samples both before and after exposure to the X-ray beam.

B. X-ray Absorption Measurements and Data Acquisition Parameters. The data were collected at the Stanford Synchrotron Radiation Laboratory under dedicated conditions (3.0 GeV, ∼50 mA). Sulfur K-edge data were measured using the 54-pole wiggler beam line 6-2 in low magnetic field mode (5 kG), a Ni-coated, flat harmonic rejection mirror, and a Si(111) double-crystal monochromator. Details of the optimization of this line for low-energy studies are described in an earlier publication.[57]

The data were collected as fluorescence excitation spectra utilizing an ionization chamber as fluorescence detector.[58,59] The energy was calibrated from the sulfur K-edge spectra of $Na_2S_2O_3 \cdot 5H_2O$ run at intervals between the samples. The maximum of the first pre-edge feature in the spectrum was assigned to 2472.02 eV. Data were collected from 2420 to 2740 eV, with a step size of 0.08 eV in the edge region. The spectrometer energy resolution was ∼0.5 eV.[57] The first and second derivatives for model compounds measured repeatedly during different experimental sessions demonstrate a reproducibility in edge position of ∼0.1 eV.

C. Data Reduction. Data from 32 scans were averaged, and a smooth pre-edge background was removed from all spectra by fitting a polynomial to the pre-edge region and subtracting this polynomial from the entire spectrum. Normalization of the data was accomplished by fitting a flat polynomial or straight line to the post-edge region and normalizing the edge jump to 1.0 at 2490 eV.

D. Fitting Procedures. The intensity of pre-edge features was quantified by fitting the data with the EDG_FIT program, which utilizes the double-precision version of the public domain MINPAK fitting library.[60] EDG_FIT was written by Dr. Graham N. George of the Stanford Synchrotron Radiation Laboratory. Pre-edge features were modeled by pseudo-Voigt line shapes fixed to have a 1:1 Gaussian/Lorentzian mixture. This line shape is appropriate as the experimental features are expected to be a convolution of the Lorentzian transition envelope[61] and the Gaussian lineshape imposed by the spectrometer optics.[58,62,63] The 1:1 Gaussian/Lorentzian admixture was found empirically to reproduce the spectral data. The number of functions

employed to fit the rising edge background was chosen on the basis of features clearly indicated by the second derivative of the data. These rising edge functions were pseudo-Voigt line shapes for which the Gaussian/Lorentzian mixture was allowed to vary to give the best empirical fit. Fits used in the calculation of pre-edge peak intensity were required to reproduce both the data and the second derivative of the data. For each spectrum, a number of fits which met these criteria were obtained. In general, fits were performed over several energy ranges, from one including only the pre-edge to one including the white line maximum of the edge. The value reported for the pre-edge intensity (where the peak area was approximated by the height × full width at half-maximum (fwhm)) is the average of all the pseudo-Voigt line shapes which successfully fit the feature. The standard deviation of the average of the areas was calculated to quantitate the uncertainty of the fit.

E. Error Analysis. There are several possible sources of systematic error in the analysis of these spectra. Normalization procedures can introduce a 1−3% difference in pre-edge peak heights, as determined by varying the parameters used to normalize a set of ligand K-edge spectra such that the final fits met requirements of consistency. This maximum of ∼3% error and the error resulting from the fitting procedure discussed above were taken into account in the calculation of pre-edge intensities and subsequent determinations of covalency.

Low-Temperature Optical Spectra. A. Sample Preparation. Protein samples (∼0.5−1.0 mM) were prepared as glasses in 50% (v/v) D_2O/glycerol-d_3 in either 50 mM phosphate (pD* 7.6) (plastocyanin) or 100 mM Tris−HCl (pD* 7.0) (T2D nitrite reductase). Protein solutions were injected *via* syringe between two quartz disks spaced by a 3.0 mm rubber gasket and secured by a Cu sample holder.

B. UV−Vis Electronic Absorption. Absorption spectra at temperatures between 5 and 300 K were obtained using a computer-interfaced Cary-17 spectrophotometer modified to accommodate a Janis Research Super Vari-Temp cryogenic dewar mounted in the light path.

C. Circular and Magnetic Circular Dichroism. Low-temperature circular dichroism and magnetic circular dichroism experiments were performed using two Jasco spectropolarimeters. Each is equipped with a modified sample compartment to accommodate focusing optics and an Oxford Instruments Spectromag 4 (SM4) superconducting magnet/cryostat which allows for data collection at temperatures from 1.6 to 290 K and fields up to 6−7 T.[64] A Jasco J-500C spectropolarimeter operating with S-1 and S-20 photomultiplier tubes for the 700−1100 and 300−800 nm regions, respectively, and an Oxford SM4-6T magnet were used to access the visible and UV spectral regions. A Jasco J-200D spectropolarimeter operating with an InSb detector and an Oxford SM4-7T magnet were used to access the near infrared region (700−2000 nm). Depolarization of the light by the MCD samples was monitored by the effect the sample had on the CD of nickel (+)-tartrate placed before and after the sample.[65] In all cases, the depolarization was less than 5%.

D. Fitting. Absorption, CD, and MCD spectra were fit to Gaussian line shapes using a modified Levenberg−Marquardt constrained nonlinear least-squares procedure.[66]

Electronic Structure Calculations. A. Active Site Geometry. The C_1(met)(his) approximation of the active sites in nitrite reductase and plastocyanin was used. In this approximation, the oxidized blue copper site is modeled by $Cu[(S(CH_3)_2)(SCH_3)(C_3N_2H_4)_2]^+$ in which dimethyl thioether replaces methionine, methyl thiolate replaces cysteine, and imidazoles replace histidine residues in the protein. No symmetry elements were imposed on the structure. The crystallographically determined coordinates[24] were used for all atoms except hydrogens, which were added to complete the site. The coordinate system for plastocyanin was chosen to position the molecule in the EPR **g**-tensor frame.[36] Nitrite reductase was placed in a coordinate system chosen to give a Cu $d_{x^2-y^2}$ ground state wave function, which is experimentally observed from the EPR spectrum ($g_{\parallel} > g_{\perp} > 2.0$).[35]

To reduce the computational effort required for calculations on a series of sites designed to stepwise transform the plastocyanin structure

(56) Ellefson, W. L.; Ulrich, E. A.; Krogmann, D. W. In *Methods in Enzymology*; San Pietro, A., Ed.; McGraw-Hill: New York, 1980; Vol. 69, pp 223−228.

(57) Hedman, B.; Frank, P.; Gheller, S. F.; Roe, A. L.; Newton, W. E.; Hodgson, K. O. *J. Am. Chem. Soc.* **1988**, *110*, 3798−3805.

(58) Lytle, F. W.; Greegor, R. B.; Sandstrom, D. R.; Marques, E. C.; Wong, J.; Spiro, C. L.; Huffman, G. P.; Huggins, F. E. *Nucl. Instr. Meth.* **1984**, *226*, 542−548.

(59) Stern, E. A.; Heald, S. M. *Rev. Sci. Instrum.* **1979**, *50*, 1579−1582.

(60) Argonne National Laboratory, B. S. Garbow, K. E. Hillstrom, J. J. More.

(61) Agarwal, B. K. *X-ray Spectroscopy*; Springer-Verlag: Berlin, 1979; pp 276 ff.

(62) Lytle, F. W. In *Applications of Synchrotron Radiation*; Winick, H., Xian, D., Ye, M.-h., Huang, T., Eds.; Gordon & Breach: New York, 1989; p 135.

(63) Tyson, T. A.; Roe, A. L.; Frank, P.; Hodgson, K. O.; Hedman, B. *Phys. Rev. B* **1989**, *39A*, 6305−6315.

(64) Allendorf, M. D.; Spira, D. J.; Solomon, E. I. *Proc. Natl. Acad. Sci. U.S.A.* **1985**, *82*, 3063−3067.

(65) Browett, W. R.; Fucaloro, A. F.; Morgan, T. V.; Stephens, P. J. *J. Am. Chem. Soc.* **1983**, *105*, 1868−1872.

(66) Press, W. H.; Flannery, B. P.; Teukolsky, S. A.; Vetterling, W. T. In *Numerical Recipes, the Art of Scientific Computing*; Cambridge University Press: Cambridge, 1988; Chapter 14.

into the nitrite reductase structure, the C_1(met)[42] approximation of the active sites in nitrite reductase and plastocyanin was also used. This approximation employs the same ligand set as the C_1(met)(his) model except amines (NH_3) are used instead of imidazoles for histidine residues. The geometries for these sites, which are described in the text, were generated using Chem 3D Plus software from Cambridge Scientific Computing. Complete tables listing Cartesian coordinates and input parameters for all calculations performed in this study are provided as supporting information.

B. SCF-Xα-SW Calculations. IBM 3BT-RS/6000 computers were used to implement the 1982 QCPE release of the SCF-Xα-SW package.[67−70] Atomic exchange parameters, α, were taken from Schwarz,[71] and the inner and outer sphere α values were determined as the valence-electron-weighted average of the atomic α values. Atomic sphere radii previously adjusted to reproduce the experimental ground state g values in plastocyanin were employed for all calculations:[41] Cu, 2.95 bohr; S(thiolate), 2.50 bohr; S(thioether), 2.30 bohr; N, 1.90 bohr; C, 1.80 bohr; and H, 1.17 bohr. A Watson sphere with radius equal to that of the outer sphere and charge equal but opposite to that of the molecule was included for ionic species. Calculations were considered converged when the maximum relative change in the atomic potentials between successive iterations was found to be less than 10^{-4} Ry, which generally required 300−400 iterations.

C. LCAO Density Functional Calculations. Calculations were performed using version 1.1.3 of the commercially distributed Amsterdam Density Functional (ADF) programs of Baerends and co-workers.[72] The Vosko−Wilk−Nusair local density approximation[73] for the exchange and correlation energy was used. The nonlocal gradient corrections of Becke[74] and Perdew[75] were included for exchange and correlation, respectively. Basis functions, core expansion functions, core coefficients, and fit functions for all atoms were used as provided from database IV, which includes Slater-type orbital triple-ζ basis sets for all atoms and a single-ζ polarization function for all atoms except Cu in this study. All core levels were treated as frozen orbitals and kept orthogonal to the valence orbitals. The numerical integration precision parameter, accint, was set to 3.5. Calculations were accepted as converged when the maximum element in the error matrix, which is defined as the commutator of the Fock matrix and the density matrix, was less than 10^{-5}.

Results and Analysis

Sulfur K-Edge XAS: Ground State Covalency. The S K-edge (S 1s → S 3p) X-ray absorption spectra of native nitrite reductase and plastocyanin[39] (as a reference), normalized to an edge jump of one sulfur, are shown in Figure 2. The K-edge absorption of a ligand such as sulfur bound to a d^9 copper ion exhibits a well-defined pre-edge feature which is assigned as a ligand 1s → ψ^* transition, where ψ^* is the half-filled HOMO on Cu(II).[76] Due to the localized nature of the S 1s orbital, this transition can have absorption intensity only if the half-filled HOMO contains a significant component of S 3p character as a result of covalency, *i.e.*, $\psi^* = (1 - \alpha'^2)^{1/2}$[Cu 3d] $- \alpha'$[S 3p], where α'^2 represents the amount of S 3p character in the HOMO.[76] The observed pre-edge transition intensity is simply the intensity of the pure electric dipole allowed S 1s → S 3p
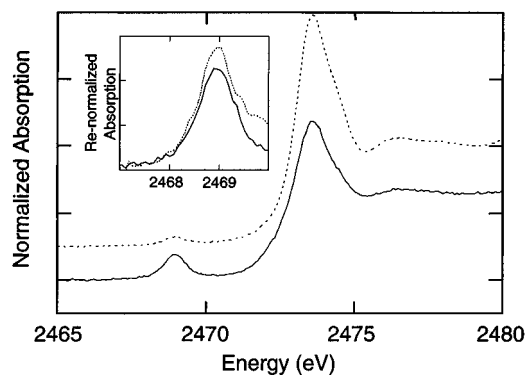
Figure 2. S K-edge X-ray absorption spectra of *A. cycloclastes* nitrite reductase (—) and spinach plastocyanin for reference (- - -). Each spectrum exhibits a single pre-edge feature at ∼2469.0 eV well separated from the rising edge. The inset shows the pre-edge regions of the spectra renormalized by a factor of 3 and 10 for plastocyanin and nitrite reductase, respectively, to account for noncoordinating sulfurs (see the text). Plastocyanin data are adapted from ref 39.

transition weighted by α'^2.

$$I(\text{S } 1s \rightarrow \psi^*) = \alpha'^2 I(\text{S } 1s \rightarrow \text{S } 3p) \qquad (1)$$

Thus, the pre-edge intensity provides a direct probe of the ligand contribution to the HOMO due to bonding.[39,76,77] Both spectra in Figure 2 exhibit a well-resolved pre-edge feature at 2469.0 eV. Only sulfurs which overlap with the Cu $3d_{x^2-y^2}$ orbital will contribute to the pre-edge intensity. In the plastocyanin[25] and nitrite reductase[24] active sites, S(Cys) and S(Met) are coordinated to the Cu and can potentially contribute to the sulfur covalency in the HOMO; however, studies on plastocyanin have shown that, due to the thioether orientation along the z axis and long Cu−S(Met) bond, only S(Cys) character is present in the $d_{x^2-y^2}$-based HOMO.[36] To compare intensities between sites, each pre-edge must be scaled (renormalized by multiplying the pre-edge by the total number of sulfurs in the protein) to account for the noncontributing sulfurs in the sample (plastocyanin contains a total of three sulfur-containing residues[78] and nitrite reductase has a total of ten sulfur-containing residues[79] per monomer). Figure 2, inset, shows the renormalized pre-edge features for plastocyanin and nitrite reductase. The renormalized intensity of these pre-edge features is qualitatively similar for both proteins, and fitting the renormalized data yields a pre-edge intensity of 1.05 ± 0.04 for nitrite reductase versus 1.02 ± 0.03 for plastocyanin.

Previously, the HOMO covalency associated with the S(Cys)−Cu interaction in plastocyanin has been quantitatively determined from S K-edge XAS to be 38 ± 1.2% S(Cys) 3p character.[39] Using this value for α'^2 and the fitted pre-edge intensity listed above for plastocyanin as a calibration of the S K-edge pre-edge intensity, the sulfur covalency in the nitrite reductase HOMO can be calculated from the renormalized experimental intensity using eq 1. From this method, the sulfur character in the HOMO of the blue copper center in nitrite reductase is found to be 39.1 ± 1.4%.

X-ray crystallographic data have indicated that the Cu−S(Cys) bond in nitrite reductase[24] (2.17 Å) is longer than in plastocyanin[25] (2.07 Å). Additionally, resonance Raman studies have shown that the principal Cu−S(Cys) stretching frequency,

(67) Johnson, K. H.; Norman, J. G., Jr.; Connolly, J. W. D. In *Computational Methods for Large Molecules and Localized States in Solids*; Herman, F., McLean, A. D., Nesbet, R. K., Eds.; Plenum: New York, 1973; pp 161−201.

(68) Connolly, J. W. D. In *Modern Theoretical Chemistry*; Segal, G. A., Ed.; Plenum: New York, 1977; Vol. 7, pp 105−132.

(69) Rosch, N. In *Electrons in Finite and Infinite Structures*; Phariseu, P., Scheire, L., Eds.; Wiley: New York, 1977.

(70) Slater, J. C. *The Calculation of Molecular Orbitals*; John Wiley & Sons: New York, 1979.

(71) Schwarz, K. *Phys. Rev. B* **1972**, *5*, 2466−2468.

(72) te Velde, G.; Baerends, E. J. *J. Comput. Phys.* **1992**, *99*, 84−98.

(73) Vosko, S. H.; Wilk, L.; Nusair, M. *Can. J. Phys.* **1980**, *58*, 1200−1211.

(74) Becke, A. D. *Phys. Rev. A* **1988**, *38*, 3098−3100.

(75) Perdew, J. P.; Wang, Y. *Phys. Rev. B* **1986**, *33*, 8800−8802.

(76) Hedman, B.; Hodgson, K. O.; Solomon, E. I. *J. Am. Chem. Soc.* **1990**, *112*, 1643−1645.

(77) Shadle, S. E.; Hedman, B.; Hodgson, K. O.; Solomon, E. I. *Inorg. Chem.* **1994**, *33*, 4235−4244.

(78) Boulter, D.; Haslett, B. G.; Peacock, D.; Ramshaw, J. A. M.; Scawen, M. D. In *International Review of Biochemistry*; Northcote, D. H., Ed.; University Park Press: Baltimore, 1977; Vol. 13, pp 1−40.

(79) Fenderson, F. F.; Kumar, S.; Adman, E. T.; Liu, M.-Y.; Payne, W. J.; LeGall, J. *Biochemistry* **1991**, *30*, 7180−7185.
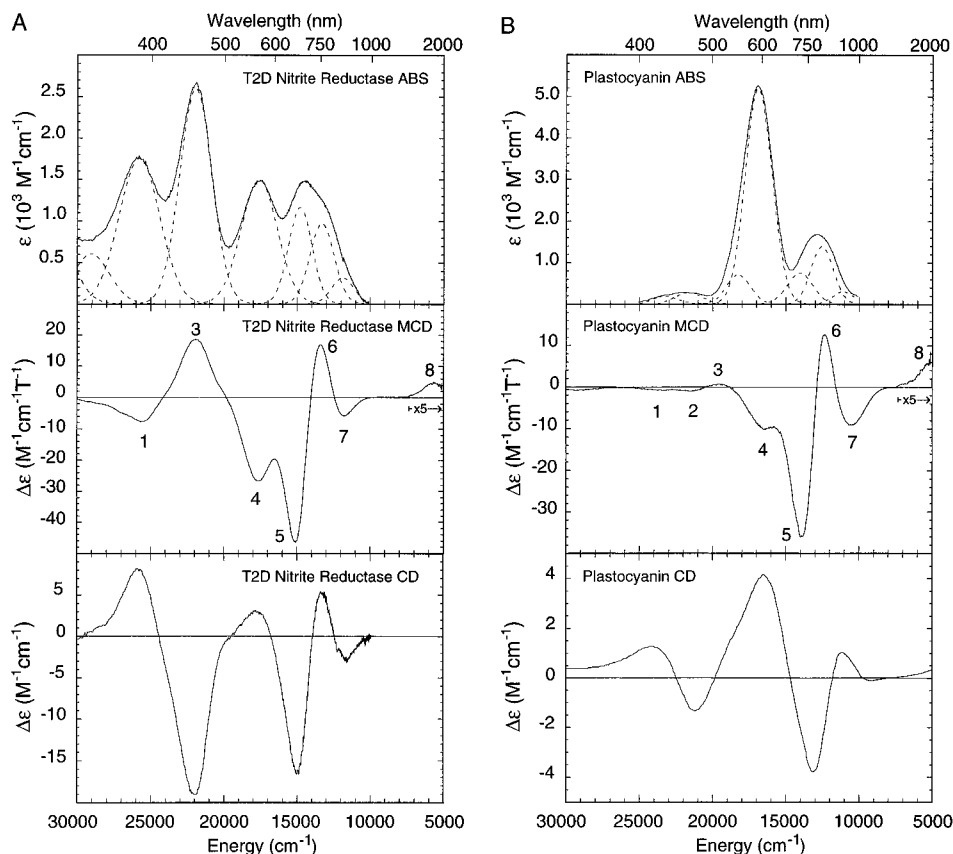
Figure 3. Electronic absorption (top), magnetic circular dichroism (middle), and circular dichroism (bottom) spectra of type 2 depleted (T2D) *A. cycloclastes* nitrite reductase (A) and spinach plastocyanin for reference (B). Nitrite reductase data are scaled to represent the signal per monomer of the trimeric protein to show the contribution of a single Cu site. Nitrite reductase spectra were obtained on 0.1 M Tris—HCl (pD* 7.0)/glycerol-d_3 glasses (50:50 v/v) at 120 K (absorption (Abs)) and 4.2 K (MCD and CD). Absorption data for plastocyanin (taken from ref 37) were recorded on a thin film at 25 K. Plastocyanin MCD and CD spectra were obtained at 4.2 K on 0.05 M phosphate (pD* 7.6)/glycerol-d_3 glasses (50:50 v/v). Gaussian resolution of bands in the absorption spectra is based on a simultaneous linear least-squares fit of the Abs, MCD, and CD data for each complex. MCD data from 5000 to 8000 cm^{-1} have been multiplied by a factor of 5. The numbering scheme is chosen to be consistent with the assignment of bands in plastocyanin (see Table 1 for assignments). A counterpart for band 2 in nitrite reductase cannot be resolved from the spectra; however, it is likely that band 2 is obscured by bands 1 and 3. Bands to higher energy than band 1 in the nitrite reductase spectra are necessary but are not labeled as they have no numbered counterpart in the plastocyanin data.

ν(Cu—S), is significantly lower in nitrite reductase[80,81] (360 cm^{-1}) than in plastocyanin[82,83] (420 cm^{-1}) which implies that the Cu—S(Cys) bond is weaker. If all the S K-edge pre-edge intensity were to arise from the S(Cys)—Cu interaction, the longer, weaker Cu—S(Cys) bond should result in less sulfur covalency in the HOMO; however, reduced sulfur covalency in nitrite reductase is not observed. Therefore, because S K-edge XAS pre-edge intensity represents the total sulfur covalency in the HOMO, S(Met) character must be mixing into the HOMO. This mixing of S(Met) character into the HOMO is likely to derive from the shorter Cu—S(Met) bond coupled with the distorted geometry in nitrite reductase compared with plasto-cyanin. This description of the changes in the Cu—S interactions in nitrite reductase relative to plastocyanin is supported by low-temperature optical spectroscopies and molecular orbital calculations (*vide infra*).

Absorption, Circular Dichroism, and Magnetic Circular Dichroism: Assignment of Ligand Field and Charge Transfer Transitions. Low-temperature absorption, MCD, and CD

(80) Han, J.; Loehr, T. M.; Lu, Y.; Valentine, J. S.; Averill, B. A.; Sanders-Loehr, J. *J. Am. Chem. Soc.* **1993**, *115*, 4256—4263.

(81) Dooley, D. M.; Moog, R. S.; Liu, M.-Y.; Payne, W. J.; LeGall, J. *J. Biol. Chem.* **1988**, *263*, 14625—14628.

(82) Han, J.; Adman, E. T.; Beppu, T.; Codd, R.; Freeman, H. C.; Huq, L.; Loehr, T. M.; Sanders-Loehr, J. *Biochemistry* **1991**, *30*, 10904—10913.

(83) Qiu, D.; Dong, S.; Ybe, J. A.; Hecht, M. H.; Spiro, T. G. *J. Am. Chem. Soc.* **1995**, *117*, 6443—6446.

spectra in the region from 5000 to 30 000 cm^{-1} for T2D nitrite reductase are presented in Figure 3A, with plastocyanin data included in Figure 3B as a reference. Data have been reported previously for plastocyanin;[37,38,41] however, instrument limita-tions precluded collecting low-temperature MCD data at energies below 9000 cm^{-1}. Also, the high-energy region (>22 500 cm^{-1}) of the MCD spectrum obtained in earlier studies was obscured by heme contamination which was identified through its relatively large $g_{||} \approx 2.8$ value compared with that of Cu(II). Plastocyanin spectra are provided in this study to extend into these regions and to facilitate comparison of the perturbed type 1 spectral features in nitrite reductase to the classic features in plastocyanin. Gaussian resolutions of the absorption spectra for plastocyanin and nitrite reductase, obtained from a simul-taneous fit of the absorption, MCD, and CD spectra for each protein, are included in the top panels of Figure 3. Low-temperature absorption spectra have been collected to 5 K for T2D nitrite reductase (120 K data are presented here because cracks in the samples at lower temperatures reduced the data quality; however, comparison of the 120 K data with 5 K data shows that the bands do not change significantly over this temperature range). Energies and ϵ values for the absorption bands determined from the fits are summarized in Table 1. The numbering scheme employed here to identify bands, which is based on a correlation of CD and MCD selection rules (*vide infra*), is the same as that used for plastocyanin.[36,41]

Table 1. Experimental Spectroscopic Parameters for Spinach Plastocyanin and *A. cycloclastes* Nitrite Reductase

band	assignments in plastocyanin[41]	energy (cm⁻¹)			ε (M⁻¹ cm⁻¹)		f		Δε (M⁻¹ cm⁻¹ T⁻¹) at 4.2 K		C_0/D_0	
		Pc	NiR	diff[a]	Pc	NiR	Pc	NiR	Pc	NiR	Pc	NiR
8	d_{z^2}	5000	5600	600					(+)[c]	+1.0	(+)[c]	(+)[c]
7	d_{xy}	10800	11900	1100	250	310	0.0031	0.0026	−8.5	−8.0	−0.213	−0.161
6	d_{xz+yz}	12800	13500	700	1425	970	0.0114	0.0086	+20.9	+23.3	+0.092	+0.150
5	d_{xz-yz}	13950	14900	950	500	1160	0.0043	0.0101	−41.4	−46.9	−0.518	−0.253
4	Cys π	16700	17550	850	5160	1490	0.0496	0.0198	−10.2	−26.8	−0.012	−0.112
3	pseudo-σ	18700	21900	3200	600	2590	0.0048	0.0299	+1.2	+18.5	+0.013	+0.044
2	His $π_1$	21390	b		288	b	0.0035	b	−0.5	b	−0.011	
1	Met a_1	23440	25650	2210	250	1750	0.0030	0.0261	−0.5	−7.5	−0.013	−0.027

[a] Difference in transition energies (defined as nitrite reductase energy minus plastocyanin energy). [b] While the presence of additional charge transfer transitions is likely based on the plastocyanin spectra, the parameters for this band in nitrite reductase cannot be determined from the data. [c] Only signs can be determined from the data for these parameters; however, the C_0/D_0 ratios should be greater than 0.1 on the basis of the relative magnitude of MCD to upper ε limit in absorption.

Experimental oscillator strengths, f_{exp}, have been calculated according to the approximation

$$f_{exp} \approx 4.61 \times 10^{-9} \epsilon_{max} \bar{\nu}_{1/2} \qquad (2)$$

where the absorption maximum, ϵ_{max}, is expressed in M^{-1} cm⁻¹ and $\bar{\nu}_{1/2}$, the full width at half-maximum of the absorption band, in cm⁻¹. The experimental oscillator strengths are given in Table 1. A useful parameter for the study of transition metal sites in proteins is the ratio of C_0, the parameter associated with MCD C-term intensity, and the dipole strength (D_0) which is related to absorption intensity.[84] Importantly, C_0/D_0 ratios allow for a differentiation of ligand field and charge transfer transitions as they are sensitive to the different selection rules for absorption and MCD spectra.[41] At low temperatures, paramagnetic Cu-(II) complexes typically exhibit MCD due only to C-term intensity, which is easily identifiable due to its $1/T$ dependence in the linear region of the magnetization-saturation curve. All features in the MCD spectra of nitrite reductase and plastocyanin presented here consist of C-term intensity and have magnetization-saturation curves that can be fit to an isotropic $g \approx 2.1$, which is indicative of a Cu(II) ground state. For complexes exhibiting only C-term MCD intensity, C_0/D_0 ratios can be determined from the Gaussian fit of the MCD spectrum taken within the linear $1/T$ region and the absorption spectrum[84] *via*

$$\frac{C_0}{D_0} = \frac{kT}{\mu_B B}\left(\frac{\Delta\epsilon}{\epsilon}\right)_{max} \qquad (3)$$

where T is the temperature, B is the external magnetic field strength, k is Boltzmann's constant, μ_B is the Bohr magneton, ϵ is the absorption maximum in M^{-1} cm⁻¹, and $\Delta\epsilon$ is the MCD intensity maximum measured in M^{-1} cm⁻¹ (note that $k/\mu_B \approx$ 1.489 T K⁻¹). The $\Delta\epsilon$ from the MCD fits and associated C_0/D_0 ratios are listed in the final columns of Table 1. For a transition to have MCD C-term intensity, it must have transition dipole moments along two principal directions of the absorption tensor.[84] The low symmetry of the blue copper site results in all transitions being electric dipole allowed; however, it also removes all orbital degeneracy. Therefore, all optical transitions will exhibit absorption intensity polarized in only one direction. These transitions can gain MCD C-term intensity through spin−orbit coupling, which mixes in orthogonal transition moment character. Therefore, the MCD intensities and hence C_0/D_0 ratios will depend on the magnitude of spin−orbit coupling occurring at the centers involved in the transitions. According to the rationale presented in ref 41, since the spin−orbit coupling parameter for Cu is greater than that for S or N (ξ_{3d}(Cu) $\approx$ 828 cm⁻¹ > ξ_{3p}(S) $\approx$ 382 cm⁻¹ > ξ_{2p}(N) $\approx$ 70 cm⁻¹), the d → d

transitions, which are centered on the Cu ion, will exhibit greater C_0/D_0 ratios than the charge transfer transitions. For plastocyanin, bands 5−8 have $|C_0/D_0| \approx 0.1$ while bands 1−4 exhibit $|C_0/D_0| \approx 0.01$;[41] therefore, the former set were assigned as d → d transitions, and the latter set were attributed to charge transfer transitions. Specific assignments for the transitions were made on the basis of the sign and magnitude of C_0/D_0 (combined with polarized absorption data), and these assignments are given in the first column of Table 1.[41]

In the low-energy region of the spectra for nitrite reductase (<16 000 cm⁻¹), four transitions (bands 5−8) are easily resolvable from the signed MCD and CD spectra (Figure 3A); these exhibit the largest $|C_0/D_0|$ ratios (Table 1). The low energy and large $|C_0/D_0|$ ratios for these bands in parallel with bands 5−8 in plastocyanin allow them to be assigned as ligand field transitions. It should be noted that while C_0/D_0 for band 8 cannot be determined from the data, estimates for the lower limit of Δε (>1.0 M^{-1} cm⁻¹ T⁻¹) and the upper limit for ε (<50 M^{-1} cm⁻¹) indicate that the lower limit of $|C_0/D_0|$ for this band is greater than 0.1. In contrast to plastocyanin, five bands (4−8) in the nitrite reductase spectra have $|C_0/D_0| > \sim 0.1$. Since mononuclear cupric complexes can exhibit, at most, four d → d transitions, one of these bands must be a charge transfer transition. Band 4 in nitrite reductase is assigned as a charge transfer transition due to its higher energy and lower C_0/D_0 ratio relative to those of bands 5−8 and its similarity in energy (and CD and MCD sign) to band 4 in plastocyanin. The CD and MCD band shape in the ligand field region for nitrite reductase is qualitatively very similar to that for plastocyanin. Bands 5−8 in nitrite reductase exhibit the same signs (negative, positive, negative, positive from high to low energy) in the MCD and CD spectra as in plastocyanin (Figure 3); therefore, the specific assignments for bands 5−8 in nitrite reductase are the same as those for bands 5−8 in plastocyanin (Table 1). All the d → d transitions in nitrite reductase have shifted by ∼1000 cm⁻¹ to higher energy than their counterparts in plastocyanin. The energies of d → d transitions are very sensitive to the ligand field at the copper center. The similar shift of all bands to higher energy indicates that the geometric differences between the sites result in an increased ligand field strength in nitrite reductase relative to plastocyanin, as would result from a tetragonal geometric distortion from pseudotetrahedral toward square planar.

In addition to the changes in ligand field energies, the Gaussian fit of the absorption spectrum of nitrite reductase reveals that there is also a redistribution of the intensity of the ligand field absorption bands. Most significantly, band 6, which is the most intense ligand field transition in the plastocyanin absorption spectrum, is reduced in intensity, while band 5 shows a corresponding increase in intensity and becomes the most

(84) Piepho, S. B.; Schatz, P. N. *Group Theory in Spectroscopy: With Applications to Magnetic Circular Dichroism*; John Wiley & Sons: New York, 1983.

Table 2. Results of SCF-Xα-SW Calculations for the Highest Occupied Valence Orbitals of the C_1(met)(his) Site in Plastocyanin and Nitrite Reductase

site	level[a]	orbital label	energy (eV)[a]	%Cu [% Cu d orbital breakdown][d]									% Cys		% Met		% His	
				Cu[b]	s[c]	p[c]	d[e]	[d_{z²}	+ d_{xz}	+ d_{yz}	+d_{x²−y²}	+ d_{xy}]	S	Cys[e]	S	Met[e]	N[f]	His[e]
Pc	48a	Cu $d_{x²−y²}$	−2.38	54	1	1	52	0.2	0.2	0.3	51.0	0.3	35	3	0	0	7	1
NiR	48a		−3.03	54	1	3	48	1.5	0.3	0.4	45.7	0.1	28	2	6	0	7	1
Pc	47a	Cu d_{xy}	−2.90	69	6	8	54	14.3	5.4	1.0	0.6	32.8	18	2	6	0	2	2
NiR	47a		−3.40	43	1	6	35	0.0	12.8	6.6	0.1	15.5	37	3	9	1	1	2
Pc	46a	Cu $d_{z²}$	−3.49	78	0	3	75	42.7	12.6	2.6	0.3	16.7	1	1	11	1	3	3
NiR	46a		−4.17	41	0	3	38	15.3	9.1	0.2	5.8	7.6	4	0	3	0	10	41
Pc	45a	Cu d_{xz+yz}	−3.65	84	0	3	81	6.4	3.0	65.0	5.0	1.5	6	1	0	0	3	4
NiR	44a		−4.29	65	1	4	60	3.3	3.8	52.0	0.7	0.2	4	3	3	0	6	18
Pc	44a	Cu $d_{xz−yz}$	−3.73	80	0	1	79	0.8	55.1	8.9	0.0	14.2	6	2	1	0	3	8
NiR	43a		−4.44	72	2	3	67	5.5	38.0	4.5	9.8	9.3	9	2	1	0	3	13
Pc	43a	His $π_1$	−4.15	13	0	2	10	0.0	4.4	0.6	4.9	0.0	7	0	1	0	11	66
NiR	45a		−4.26	26	2	2	23	6.7	3.3	0.5	0.5	12.0	1	0	12	2	10	46
Pc	42a	Cys $π$	−4.26	49	0	5	42	0.2	11.6	5.6	23.9	0.7	30	4	1	0	3	14
NiR	41a		−4.86	65	0	2	62	7.8	26.4	2.1	8.8	16.8	17	3	1	0	2	12
Pc	41a	Met b_1	−4.43	26	3	1	22	21.0	0.5	0.1	0.3	0.1	0	0	59	12	0	2
NiR	40a		−4.90	46	1	1	43	3.6	24.9	2.4	3.3	8.8	1	0	35	9	0	6
Pc	40a	His $π_1$	−4.57	12	0	0	11	0.4	0.0	8.8	1.4	0.4	2	0	0	0	7	76
NiR	42a		−4.56	41	1	1	38	9.8	2.7	13.1	3.1	9.2	6	1	12	4	3	33
Pc	39a	Cys pseudo-$σ$	−5.29	38	2	5	30	5.7	0.0	0.0	0.0	24.2	51	8	0	0	1	0
NiR	39a		−5.70	37	2	5	29	5.5	0.1	5.6	4.5	13.3	49	9	0	0	2	1
Pc	38a	His $π_2$	−6.19	6	0	0	5	1.7	1.7	0.0	0.0	1.3	0	0	10	5	41	35
NiR	38a		−6.41	11	0	0	10	0.1	6.4	0.9	0.0	2.6	2	0	0	0	46	39
Pc	37a	Met a_1	−6.44	5	0	1	4	1.4	1.7	0.4	0.2	0.4	0	0	49	29	9	7
NiR	36a		−6.90	10	1	3	9	2.6	3.7	0.8	0.8	1.1	0	0	46	32	6	5
Pc	36a	His $π_2$	−6.78	8	0	1	5	0.0	0.0	3.5	0.0	1.5	0	0	2	5	48	37
NiR	37a		−6.55	8	0	0	7	1.9	0.2	0.3	0.0	4.6	0	0	8	4	43	35
Pc	35a	Cys $σ$	−7.68	22	1	8	11	0.1	3.4	2.4	0.1	5.0	42	27	1	2	4	0
NiR	35a		−7.54	21	2	6	13	0.4	0.3	9.1	2.8	0.4	46	29	0	0	2	0

[a] Levels are ordered according to energies in plastocyanin. [b] Total charge on the copper ion. [c] l quantum breakdown for the copper ion. [d] Specific d orbital contributions to the total Cu d charge. [e] Total charge for all atoms of the ligand except the S or N coordinated to Cu. [f] Total charge for the coordinating N atoms.

intense ligand field transition in nitrite reductase (Table 1). In plastocyanin, the high intensity of band 6, which is assigned as the Cu $3d_{xz+yz} →$ Cu $3d_{x²−y²}$ transition, is attributed to d_{xz+yz} having the correct symmetry to configurationally interact with the S(Cys) $pπ$ orbital.[41] This mixing allows for the ligand field transition to gain intensity from the highly allowed (*vide infra*) S(Cys) $pπ →$ Cu $3d_{x²−y²}$ blue band (band 4). In a similar fashion, band 5, which is assigned as the Cu $3d_{xz−yz} →$ Cu $3d_{x²−y²}$ transition, can gain intensity through symmetry-allowed mixing with the S(Cys) pseudo-$σ$ level. However, since the S(Cys) pseudo-$σ →$ Cu $3d_{x²−y²}$ transition (band 3) in plastocyanin is weak, band 5 gains little intensity. Thus, the increase in band 5 intensity and decrease in band 6 in nitrite reductase relative to plastocyanin correlate directly to an increase in the S(Cys) pseudo-$σ →$ Cu $3d_{x²−y²}$ and a decrease in the S(Cys) $pπ →$ Cu $3d_{x²−y²}$ charge transfer transition intensities. As charge transfer transition intensities are dependent on the overlap between ligand and metal orbitals, the increase in the band 5/band 6 ratio in nitrite reductase indicates that there is a decrease in the S(Cys) $π$ overlap and a corresponding increase in the pseudo-$σ$ overlap with the $d_{x²−y²}$ HOMO compared with plastocyanin.

While the ligand field region in nitrite reductase appears qualitatively similar to that in plastocyanin, the charge transfer region is dramatically different. Three bands (4, 3, and 1) can be unambiguously identified to higher energy than the ligand field transitions in nitrite reductase (Figure 3). Band 2 is not labeled in the nitrite reductase spectra because, due to overlap with bands 1 and 3, no band is observed which exhibits the CD and MCD signs associated with band 2 in plastocyanin. These bands exhibit smaller C_0/D_0 ratios than the ligand field transitions which allow for their assignment as charge transfer transitions (Table 1). However, all the charge transfer transitions in nitrite reductase have greater C_0/D_0 ratios than their counterparts in plastocyanin, especially band 4 as mentioned above

(Table 1). The origin of the increased C_0/D_0 ratios for the charge transfer transitions in nitrite reductase relative to plastocyanin can be traced to the amount of metal d character found in the ligand orbitals. While absorption intensity will be dependent on the amount of overlap between the ligand orbital and the $d_{x²−y²}$ HOMO, MCD intensity will be dependent on the total amount of Cu d character, hence spin−orbit coupling, mixed into the orbitals. Electronic structure calculations (*vide infra*, Table 2) indicate that the ligand orbitals involved in the observed charge transfer transitions contain more *total* Cu d character in nitrite reductase than in plastocyanin; *e.g.,* the S(Cys) $π$ orbital in nitrite reductase contains 62% Cu d character versus 42% in plastocyanin.

Band 4 occurs at similar energy and exhibits the same negative CD and MCD signs as the blue band in plastocyanin. In parallel, this band is assigned as the lowest energy, S(Cys) $pπ →$ Cu $3d_{x²−y²}$ charge transfer transition. The MCD spectrum of plastocyanin only exhibits one positive band in the charge transfer region, band 3, which is assigned as the S(Cys) pseudo-$σ →$ Cu $3d_{x²−y²}$ transition. Correspondingly, the single positive charge transfer feature in the nitrite reductase MCD, band 3, is assigned to this transition. In comparison to plastocyanin, a significant redistribution of absorption intensities between bands 3 and 4 in nitrite reductase is observed. The S(Cys) $pπ →$ Cu $3d_{x²−y²}$ transition in nitrite reductase is ~3 times weaker than its counterpart in plastocyanin, which is the dominant absorption feature, and the dramatic drop in intensity for this band is accompanied by a corresponding increase in intensity for the higher energy S(Cys) pseudo-$σ →$ Cu $3d_{x²−y²}$ transition, which becomes the dominant absorption feature in nitrite reductase. Since the intensity of these charge transfer transitions is proportional to the overlap of the cysteine and Cu $d_{x²−y²}$ orbitals, the gain in intensity for band 3 and the loss of intensity for band 4 relative to those of plastocyanin indicate a decrease in $π$ overlap and increase in pseudo-$σ$ overlap in the nitrite

reductase HOMO. These changes in the σ and π bonding in the nitrite reductase site are consistent with the absorption intensity redistribution in the ligand field transitions (band 5 and 6) presented above. Also, the total oscillator strength for the cysteine-based charge transfer transitions is smaller in nitrite reductase (0.0497) than in plastocyanin (0.0544) which indicates that in addition to a shift in the π/σ overlap involving the S(Cys), the total S(Cys) contribution to the HOMO is less in nitrite reductase. This finding is consistent with the reduced S(Cys) covalency in the HOMO expected from crystallographic[24] and resonance Raman[80] studies and further supports the implication from S K-edge XAS that an additional sulfur, *i.e.,* S(Met), must be contributing to the HOMO.

The transitions to higher energy than the cysteine-based charge transfer transitions in nitrite reductase bear little resemblance to the high-energy region in plastocyanin. While the plastocyanin MCD spectrum exhibits two transitions, assigned as His $\pi_1 \rightarrow$ Cu $3d_{x^2-y^2}$ and Met $a_1 \rightarrow$ Cu $3d_{x^2-y^2}$ charge transfer transitions, which are weak in both absorption and MCD spectra, the nitrite reductase MCD spectrum consists of a single resolvable band with appreciable MCD and absorption intensity. Both of the transitions in plastocyanin have negative MCD signs; however, His $\pi_1 \rightarrow$ Cu $3d_{x^2-y^2}$ is negative and Met $a_1 \rightarrow$ Cu $3d_{x^2-y^2}$ is positive in the plastocyanin CD spectrum. Band 1 in nitrite reductase has a negative MCD and a positive CD sign, and is therefore assigned as a Met $\rightarrow$ Cu $3d_{x^2-y^2}$ transition. The large absorption intensity associated with band 1 in nitrite reductase reflects the fact that significant S(Met) character is present in the nitrite reductase HOMO which accounts for the additional sulfur covalency indicated by the S K-edge data. A His $\pi_1 \rightarrow$ Cu $3d_{x^2-y^2}$ transition, analogous to band 2 in plastocyanin, cannot be resolved from the nitrite reductase data; however, this band would be obscured by the increased intensity of bands 1 and 3.

Electronic Structure Calculations: Bonding in Nitrite Reductase. Previously, SCF-Xα-SW calculations for plastocyanin[41,42,55] have been performed utilizing the C_s(met) and C_s-(met)(his) active site approximations in which the geometry of the site is modified slightly to incorporate a mirror plane containing Cu, S(Cys), and S(Met). However, as can be seen in Figure 1B, imposition of a mirror plane into the type 1 active site of nitrite reductase would require significant geometric changes to the site, particularly with respect to the S(Cys)−Cu−S(Met) plane which tilts such that it is no longer approximately perpendicular to the N(His)-Cu-N(His) plane (as in plastocyanin). In order to accurately investigate the changes in the electronic structure which arise from the geometric distortions in nitrite reductase relative to plastocyanin, the C_1-(met)(his) approximation has been used in this study. This approximation, in which the crystallographic coordinates for all atoms except hydrogens are used, imposes no symmetry elements on the site and thus retains its C_1 symmetry. Furthermore, while prior studies on plastocyanin have shown that substitution of amines and imidazoles for His residues in SCF-Xα-SW calculations yields similar results[41,42] (and therefore amines have been utilized in most calculations on blue copper sites), this was not presumed to be the case for nitrite reductase. Because the perturbed spectral features of nitrite reductase include marked changes in the charge transfer region, imidazoles have been used in the C_1(met)(his) approximation to allow for the possible observation of increased His−Cu interactions which may lead to greater His to Cu charge transfer intensity.

The ground state energies and one-electron wave functions for the highest occupied valence orbitals obtained from SCF-Xα-SW calculations on the C_1(met)(his) approximation of the

nitrite reductase and plastocyanin active sites are presented in Table 2. The results for plastocyanin are very similar to those reported for the C_s(met) and C_s(met)(his) approximations.[41,55] The plastocyanin $d_{x^2-y^2}$ HOMO (level 48a) is highly covalent (52% Cu d character), with the predominant Cu−ligand interaction involving 35% S(Cys) and a minor contribution from the coordinating N(His) atoms (7% total). While these values differ to a limited extent from those reported previously from theory[41] and experiment[39,40] ($\sim$42% Cu d, 36−38% S p, and 4% N) due to effects of partitioning the charge found in the intersphere region, the present calculations are appropriate for examination of the differences in bonding between plastocyanin and nitrite reductase. Compared with plastocyanin, the nitrite reductase HOMO (level 48a) is also highly covalent (48% Cu d character); however, the amount of S(Cys) covalency in the HOMO is reduced (28%). The amount of coordinating N(His) contribution to the HOMO in nitrite reductase (7% total) does not change which indicates that significant changes in Cu−His bonding involving this orbital do not occur. On the other hand, the amount of S(Met) character in the nitrite reductase HOMO (6%) is increased relative to the plastocyanin HOMO, which exhibits virtually no S(Met) contribution.[41]

The changes in the HOMO wave functions calculated for nitrite reductase and plastocyanin are entirely consistent with the description of the sulfur covalency developed from the S K-edge data. While the S(Cys) covalency in nitrite reductase is substantially reduced relative to that in plastocyanin, the total sulfur covalency remains unchanged ($\sim$35% in both systems). The total sulfur covalency remains the same because the loss in covalency from S(Cys) is compensated for by the dramatic increase in covalency involving the S(Met). This presence of significant S(Met) character indicates that an important new ligand−metal interaction involving the methionine occurs in the nitrite reductase active site.

This description of the covalency in the nitrite reductase HOMO coupled with the experimental ligand field transition energies (bands 5−8 in Table 1) relative to those in plastocyanin allows for the origins of the perturbed EPR spectrum of nitrite reductase to be ascertained. Ligand field theory expressions[85] for the g values of a $d_{x^2-y^2}$ half-occupied HOMO indicate that the deviations of the g values from the spin-only value, 2.0023, are inversely proportional to ligand field transition energies. Thus, the shift to lower g values for nitrite reductase[18,19,35] ($g_{\parallel}$ = 2.195, $g_{\perp}$ = 2.04 versus $g_{\parallel}$ = 2.226, $g_{\perp}$ = 2.05 for plastocyanin[36]) can be attributed to the increase in the ligand field transition energies in nitrite reductase, bands 5−8 in Table 1, by $\sim$1000 cm^{-1} relative to those in plastocyanin. If the differences in the ground and excited state covalencies in nitrite reductase are considered to be negligible, the change in the g values expected from the shift in ligand field transition energies can be calculated through

$$\Delta g_{\parallel}(\text{NiR}) = \frac{E_{xy}(\text{Pc})}{E_{xy}(\text{NiR})}\Delta g_{\parallel}(\text{Pc}) \qquad (4a)$$

$$\Delta g_{\perp}(\text{NiR}) = \frac{E_{xz,yz}(\text{Pc})}{E_{xz,yz}(\text{NiR})}\Delta g_{\perp}(\text{Pc}) \qquad (4b)$$

where Δg represents the deviation of g from the spin-only value and E is the transition energy in cm^{-1}. Substitution of the experimental transition energies into eqs 4a and 4b predicts $g_{\parallel}$ = 2.203 and $g_{\perp}$ = 2.045 for nitrite reductase, which compare favorably with the experimental values above. This shift in the g values is primarily responsible for the difference in $A_{\parallel}$ in nitrite reductase ($|73| \times 10^{-4}$ cm^{-1}) relative to plastocyanin ($-63 \times$

(85) McGarvey, B. R. *Transition Met. Chem. (N.Y.)* **1966**, *3*, 89−201.
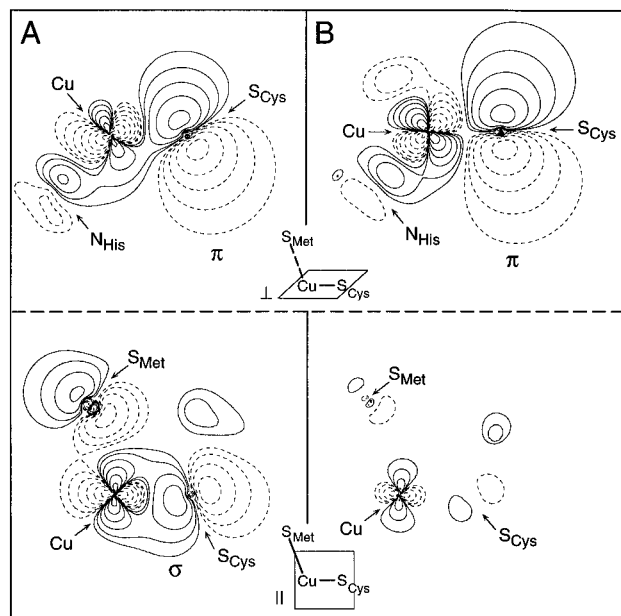
Figure 4. Contours of the highest energy, half-filled orbital for *A. cycloclastes* nitrite reductase (A) and plastocyanin (B) plotted perpendicular (top) and parallel (bottom) to the S(Cys)−Cu−S(Met) plane. Contour lines are drawn at ±0.64, ±0.32, ±0.16, ±0.08, ±0.04, ±0.02, and ±0.01 $(e^-/bohr^3)^{1/2}$.

10^{-4} cm^{-1}). Provided that the spin densities on the Cu are the same for nitrite reductase and plastocyanin (as is established above by experiment and calculations), the change in $A_\parallel$ resulting from the shift in g values can be calculated through the perturbation treatment of Abragam and Pryce[86]

$$A_\parallel(NiR) = P[(3/7)(g_\perp(NiR) - g_\perp(Pc)) + (g_\parallel(NiR) -$$
$$g_\parallel(Pc))] - A_\parallel(Pc) \quad (5)$$

where $P = 396 \times 10^{-4}$ cm^{-1}. Substituting the experimental EPR values into the above expression produces a calculated $A_\parallel$ = -77×10^{-4} cm^{-1} for nitrite reductase, which is in reasonable agreement with the experimental value, $|73| \times 10^{-4}$ cm^{-1}. It should be noted that while the geometric changes, which generate the increased ligand field strength, are responsible for the differences in the EPR g values between nitrite reductase and plastocyanin, the small hyperfine coupling in both centers is still primarily a result of a highly covalent site, not the alternative "geometry" explanation of Cu $4p_z$ mixing,[43−45] into the $d_{x^2-y^2}$ HOMO. Finally, nitrite reductase exhibits an increased rhombic splitting of its g values ($\Delta g_\perp = 0.04$)[87] compared to those of plastocyanin ($\Delta g_\perp = 0.017$).[36] Detailed studies by Gewirth *et al.*[16] have shown that rhombic splitting in the EPR spectra of distorted tetrahedral Cu(II) complexes can be attributed to d_{z^2} mixing into the $d_{x^2-y^2}$ HOMO, and that this mixing is likely to be a result of increased ligand field strength along the z (*i.e.*, axial) direction in the blue copper site. According to this analysis, 1.8% d_{z^2} character would account for the increased rhombic splitting observed for nitrite reductase. The SCF-Xα-SW calculations for nitrite reductase show that increased d_{z^2} mixing into the nitrite reductase HOMO does occur, and the magnitude (1.5% from Table 2) is sufficient to generate the rhombic splitting observed.

Contour plots for the nitrite reductase and plastocyanin HOMOs are shown in Figure 4. The dominant Cu−S(Cys) π

(86) Abragam, A.; Pryce, M. H. L. *Proc. R. Soc. London., A* **1951**, *205*, 135.
(87) Suzuki, S.; Kohzuma, T.; Deligeer; Yamaguchi, K.; Nakamura, N.; Shidara, S.; Kobayashi, K.; Tagawa, S. *J. Am. Chem. Soc.* **1994**, *116*, 11145−11146.

antibonding interaction in the classic plastocyanin HOMO is clearly evident in Figure 4B (top). Further, the lack of electron density found along the Cu−S(Cys) and −S(Met) bonds in plastocyanin (Figure 4B, bottom) illustrates that there is little S(Cys) σ or S(Met) interaction with the Cu in the HOMO. The principal change in the nitrite reductase HOMO wave function relative to that of plastocyanin involves a rotation of the Cu $d_{x^2-y^2}$ orbital by 30−35° about the molecular *z*-axis (*i.e.*, the Cu−S(Met) bond) and by a similar amount about the Cu−S(Cys) bond. This rotation results in a decrease in the π overlap (Figure 4A, top) and an increase in the σ overlap of the Cu $d_{x^2-y^2}$ and S(Cys) orbitals, which is indicated by the increased electron density along the Cu−S(Cys) bond (Figure 4A, bottom), compared with those of plastocyanin. Also, this rotation allows for Cu $d_{x^2-y^2}$ to interact with the methionine ligand (Figure 4A, bottom) and thus mixes S(Met) character into the HOMO, introducing the new source of sulfur covalency indicated by experiment.

As the charge transfer transition intensities depend on the specific ligand orbitals involved in bonding with the HOMO as well as the total ligand character, the rotation of Cu $d_{x^2-y^2}$ is important in that it provides a mechanism for the changes in charge transfer transition intensity observed experimentally. The degree to which the specific ligand orbitals mix with the HOMO is reflected in the amount of Cu $d_{x^2-y^2}$ character present in the bonding ligand derived orbitals (Table 2). The amount of Cu $d_{x^2-y^2}$ in the Cys π orbital (level 41a) in nitrite reductase is found to decrease significantly to 8.8% from 23.9% in plastocyanin (level 42a). This loss in π overlap is accompanied by an increase in the amount of Cu $d_{x^2-y^2}$ character in the Cys pseudo-σ bonding level (4.5% in nitrite reductase versus 0% in plastocyanin, level 39a in both calculations). The Cys σ orbital (level 35a) is also found to exhibit slightly increased overlap with Cu $d_{x^2-y^2}$; however, this level is at sufficiently deep binding energy that the S(Cys) pσ → Cu $3d_{x^2-y^2}$ transition will not appear in the energy range of the optical spectra presented here. The dominant contribution of the methionine ligand with Cu $d_{x^2-y^2}$ involves the Met b_1 orbital. The Met b_1 orbital in nitrite reductase (level 40a) contains 3.3% Cu $d_{x^2-y^2}$ compared with 0.3% in plastocyanin (level 41a). Compared with the Met b_1 orbital, the Met a_1 level, which is found at a deeper binding energy and was originally thought[41] to be responsible for Cu−Met bonding, undergoes significantly less interaction with $d_{x^2-y^2}$. Finally the histidines contribute mostly His σ (which is found to deeper binding energy than is presented in Table 2) character to the HOMO. In nitrite reductase, the lower energy His π_1 orbitals (levels 45a and 42a) contain a total of only ~4% $d_{x^2-y^2}$ character while the His σ levels consist of ~15% $d_{x^2-y^2}$ (the His π_2 orbitals in both plastocyanin and nitrite reductase do not have a $d_{x^2-y^2}$ contribution). The His π_1 orbitals would be at an appropriate energy to appear in the experimental spectra of nitrite reductase; however, the differences in the amount of $d_{x^2-y^2}$ character in these levels compared with those of plastocyanin indicate that the transitions in nitrite reductase would be negligibly more intense (3.1%, NiR level 42a, versus 1.4%, Pc level 40a) or less intense (0.5%, NiR level 45a, versus 4.9%, Pc level 43a) than those in plastocyanin. Thus, the changes in the bonding between nitrite reductase and plastocyanin indicate that the His → Cu $3d_{x^2-y^2}$ transitions should change negligibly in the ~28 000 cm^{-1} range. These changes in ground and excited state orbital overlaps are completely consistent with the experimentally observed intensity changes and provide considerable support for the assignments of the S(Cys) pπ and S(Cys) pseudo-σ → Cu $3d_{x^2-y^2}$ transitions in nitrite reductase and the description of the intensity redistribution involving these transitions. Further, these bonding changes strongly indicate that the

additional high-energy, intense absorption band in nitrite reductase is attributable to a Met → Cu $3d_{x^2-y^2}$ charge transfer transition.
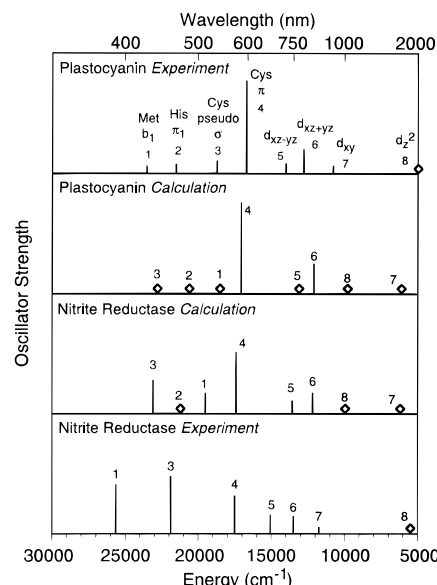
Theoretical transition energies can be obtained from density functional calculations using the method of Slater,[70] in which 0.5 electron is transferred between the ground and excited states and the transition energy is calculated as the difference between the energies of the one-electron orbitals involved in the transition. Oscillator strengths (*i.e.*, absorption transition intensities), f_{calc}, can be calculated from SCF-Xα-SW-calculated wave functions as performed in ref 41 using the ligand−ligand overlap term of van der Avoird and Ros.[88] The oscillator strength is approximated as a sum of the overlaps between ligand-centered orbitals in the ground (Φ_L) and excited state (Φ_L') molecular orbitals. Overlaps involving metal-centered orbitals, which have been shown through calculations to contribute relatively little to the oscillator strength, are neglected such that

$$f_{calc} = 1.085 \times 10^{11} (\Delta E)|D|^2 \qquad (6)$$

in which

$$D = \langle \Phi_L' | \vec{r} | \Phi_L \rangle \approx \sum_a \sum_b C'_{ab} C_{ab} \vec{r}_a \qquad (7)$$

where ΔE is the transition energy, C_{ab} and C'_{ab} are the coefficients of orbital b on ligand a for the ground and excited state molecular orbitals, respectively, and $\vec{r}$ is the position vector to ligand a. This method has been successfully applied to SCF-Xα-SW calculations on chlorocuprates[89] and plastocyanin.[41] In order to calculate the oscillator strengths and transition energy differences between nitrite reductase and plastocyanin (which are dependent on the atomic sphere sizes used in the SCF-Xα-SW formalism), without introducing the additional parameter of sphere variation,[16,41,90] calculations have also been performed on the sites using ADF density functional calculations which utilize atomic basis functions[72] rather than scattered wave solutions and thus are not dependent on sphere sizes. The calculated transition energies and oscillator strengths for nitrite and plastocyanin obtained from the ADF calculations are presented in Figure 5. The calculated transition energies and oscillator strengths for plastocyanin are very similar to those obtained previously for the C_s(met) site.[41] Importantly, the calculations reproduce all of the general features of the experimental absorption spectrum and show that the band with dominant intensity is the S(Cys) pπ → Cu $3d_{x^2-y^2}$ transition (band 4). In addition, the ligand field transitions are all predicted to be lower in energy than the charge transfer transitions, with band 6 having the greatest intensity due to the ∼15% Cys π charge transfer intensity mixed into the d_{xz+yz} → $d_{x^2-y^2}$ ligand field transition. The d_{z^2} → $d_{x^2-y^2}$ transition is predicted to be higher in energy and the d_{xy} → $d_{x^2-y^2}$ transition lower in energy, indicating that the S(Met)−Cu and the S(Cys) π−Cu bonding interactions are somewhat underestimated in the calculation. The S(Cys) pseudo-σ, Met b_1, and His π_1 → Cu $3d_{x^2-y^2}$ charge transfer transitions are all predicted to be at higher energy than band 4 and calculated to be very weak in intensity, as is observed experimentally. The Cys pseudo-σ/π splitting is calculated to be larger than observed, and the Met b_1 → Cu $3d_{x^2-y^2}$ transition is found at lower energy than observed experimentally. This is consistent with the small differences between the experimental

(88) van der Avoird, A.; Ros, P. *Theor. Chim. Acta* **1966**, *4*, 13−21.
(89) Desjardins, S. R.; Penfield, K. W.; Cohen, S. L.; Musselman, R. L.; Solomon, E. I. *J. Am. Chem. Soc.* **1983**, *105*, 4590−4603.
(90) Bencini, A.; Gatteschi, D. *J. Am. Chem. Soc.* **1983**, *105*, 5535−5541.

Figure 5. Experimental and calculated (as described in the text) transition energies and oscillator strengths for the plastocyanin and nitrite reductase active sites. Bar heights represent intensity, and diamonds indicate the energy (determined from MCD spectra) for transitions in which either the intensity has not been obtained experimentally or the calculated oscillator strength is smaller than the scale shown. The theoretical oscillator strengths have been scaled to experimental value for band 4 in plastocyanin.

and calculated Cys and Met bonding interactions with the Cu from the ligand field energy comparison.

In agreement with experiment, the calculated transitions for nitrite reductase all shift to higher energy relative to those of plastocyanin. The transition intensity changes between plastocyanin and nitrite reductase are also consistent with experiment. In the ligand field region of nitrite reductase, the oscillator strength associated with band 6 decreases while that of band 5 increases. As described above, the redistribution of intensity in the ligand field region is connected to the changes in the charge transfer region. Bands 1 and 3 increase in intensity while band 4 decreases in nitrite reductase compared to those in plastocyanin, as is observed experimentally, which indicate increased S(Cys) pseudo-σ and S(Met) mixing into the HOMO accompanied by a decrease in the S(Cys) π overlap and supports the bonding description developed above. These results indicate that the calculations correctly model the directions of the bonding changes and their effect on intensity in the absorption spectra. The actual bonding changes between the sites are found to be more extensive than those indicated by the calculations because the magnitude of the charge transfer intensity changes calculated is somewhat less than that observed from experiment. In particular, while band 4 decreases in nitrite reductase and band 3 increases significantly in intensity, the calculation indicates that band 4 should still be the most intense feature while band 3 is experimentally observed to be more intense than band 4.

Geometric Origins of the Perturbed Electronic Structure of Nitrite Reductase. In order to determine the contributions of specific geometric distortions to the changes in the electronic structure between nitrite reductase and plastocyanin, electronic structure calculations have been performed on a series of computational models designed to systematically transform the plastocyanin active site into the nitrite reductase center. The C_1(met) approximation, in which the histidines are replaced by amines, has been used in these calculations because the histidine residues have been shown from the C_1(met)(his) calculations detailed above to play a negligible role in the differences in
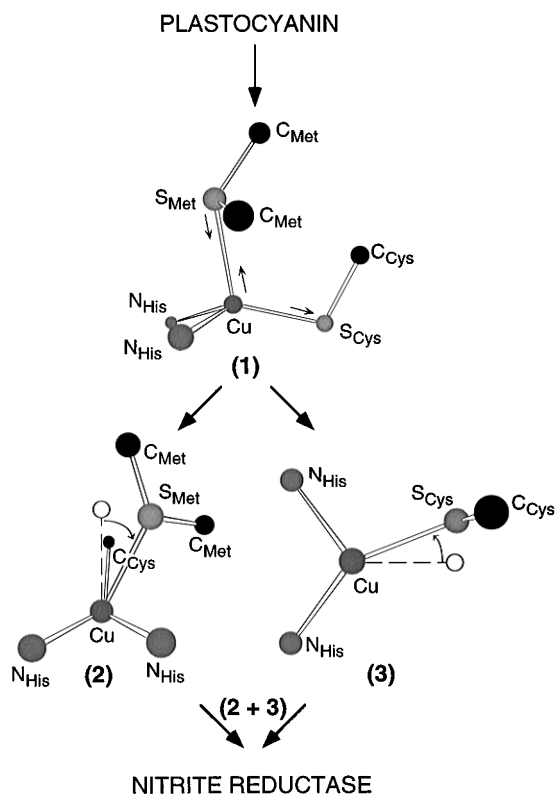
Figure 6. Geometric distortions performed to generate the computational models employed to systematically transform the plastocyanin active site structure into that of nitrite reductase. The dashed ball and sticks in models 2 and 3 indicate the atomic positions prior to distortion. Model 2 is viewed along the Cu−S(Cys) bond, and thus S(Cys) is obscured by Cu. For clarity, the methionine residue is omitted from the view provided for model 3.

bonding between nitrite reductase and plastocyanin. The distortions implemented to generate the computational models are depicted in Figure 6. Model 1 represents a distortion of the plastocyanin structure toward a more tetrahedral structure. The Cu−S(Met) bond is shortened by 0.27 Å, the Cu−S(Cys) bond is lengthened by 0.1 Å, and the Cu ion is moved further out of the equatorial NNS(Cys) plane toward S(Met) by 0.2 Å to match the distances in nitrite reductase. The angular distribution of the ligands in this model are changed very little from that in plastocyanin. In models 2 and 3, the distortions involving the angular orientation of the methionine and cysteine residues, respectively, are added to the distortions included in model 1. Model 2 incorporates the tilting of the methionine residue toward the NNS plane by 31°, and model 3 includes the rotation of the cysteine with respect to the N(His) atoms in the NNS plane by 17° observed in nitrite reductase compared with that in plastocyanin. Finally, model (2 + 3) contains all the distortions used in models 1, 2, and 3. The structure of model (2 + 3) is identical to nitrite reductase with the exception of small differences in several internal coordinates of the residues, *e.g.*, the Cu−S(Cys)−C(Cys) angle.

The changes relative to plastocyanin in the charge decompositions for the HOMOs obtained from SCF-Xα-SW calculations on the models described above are presented in Table 3. For comparison, the results of a C_1(met) calculation performed on nitrite reductase are included in the last row of Table 3. The tetrahedral distortion introduced in model 1 changes the HOMO relatively little compared with that in plastocyanin. The lengthening of the Cu−S(Cys) bond results in a small decrease in the S(Cys) character (−1.0%) accompanied by a minor increase in the S(Met) character (0.3%) in the HOMO; however, these effects are an order of magnitude smaller than those observed for nitrite reductase, in which S(Cys) character

decreases by 10.3% and S(Met) character increases by 5.8%. It should be noted that while the tetrahedral distortion present in model 1 does not reproduce the nitrite reductase HOMO (and therefore indicates that the distortion is not primarily responsible for generating the nitrite reductase spectral features), this distortion produces significant changes in electronic structure, particularly in the splitting of the $d_{x^2-y^2}$ and d_{xy} orbitals (*vide infra*). The angular distortions included in models 2 and 3 result in more pronounced changes in the S(Cys) and S(Met) character. Once again, though these changes are in the right direction with regard to nitrite reductase (model 2, −2.8% S(Cys), 1.4% S(Met); model 3, −7.3% S(Cys), 2.0% S(Met)), the magnitude of the changes introduced by each individual distortion does not account for the changes seen in nitrite reductase. However, if the distortions are allowed to occur together, model (2 + 3), the values found for nitrite reductase are obtained (−10.0% S(Cys), 5.8% S(Met)). It should be noted that the minor differences in the HOMO charge decomposition between model (2 + 3) and nitrite reductase are a result of small differences present in the internal coordinates of the residues and that the changes in the model (2 + 3) HOMO relative to that of plastocyanin are greater than the sum of the changes in models 2 and 3. *Therefore, the changes in the electronic structure in nitrite reductase relative to plastocyanin are predominantly the result of the coupled angular movement of the methionine residue toward the NNS plane and a rotation of the cysteine residue within the NNS plane.*

Discussion

The green "blue" copper site in nitrite reductase exhibits dramatically different spectroscopic features[18,19,35,80,87] compared to the classic site in plastocyanin.[13,14] Nitrite reductase exhibits all the characteristics associated with perturbed blue copper sites. Absorption intensity at ∼600 nm decreases accompanied by a increase in intensity of the absorption envelope at ∼450 nm, and the EPR spectrum of nitrite reductase is rhombic with a large $|A_x|$. Compared with plastocyanin, nitrite reductase shows increased rhombic splitting ($\Delta g_\perp = 0.04$ versus 0.017), g_z is smaller (2.19 versus 2.23), $|A_x|$ is increased (42 versus 17 × 10^{-4} cm^{-1}), and $|A_z|$ is increased (73 versus 63 × 10^{-4} cm^{-1}). Additionally, a band at ∼385 nm in the nitrite reductase absorption spectrum is unusually intense even for perturbed sites, and an extreme redistribution of the charge transfer transition intensities (the ∼450 nm band is more intense than the ∼600 nm band) occurs. These features indicate that the electronic structure of the type 1 site in nitrite reductase differs significantly from that of classic blue copper sites and may represent the limit of a large perturbation.

In this study, the highly perturbed nature of this site has been defined through S K-edge XAS, low-temperature absorption, CD, and MCD spectroscopies. S K-edge XAS has been used to probe the Cu−S interactions, which have been shown to dominate the electronic structure of plastocyanin,[41,42] in the nitrite reductase HOMO through analysis of the pre-edge energy and intensity. Despite a longer, weaker Cu−S(Cys) bond in nitrite reductase relative to plastocyanin, the pre-edge intensity, and thus sulfur covalency, and energy in nitrite reductase surprisingly remain the same as for the classic site in plastocyanin. Correlation of the signs and magnitudes of the low-temperature absorption, CD, and MCD spectra allows for the specific identification and assignment of the bands in the optical spectra of nitrite reductase to be made relative to those of plastocyanin. These assignments indicate that a redistribution of absorption intensity in the d → d transitions accompanies the changes in the charge transfer intensities. The spectra also show that all the ligand field transitions in nitrite reductase have

Table 3. Changes in the SCF-Xα-SW d$_{x^2-y^2}$ HOMO Charge Decomposition for the C_1(met) Active Sites of Geometric Models and Nitrite Reductase Relative to Plastocyanin

structure	Δ(% Cu)				Δ(% Cys)		Δ(% Met)		Δ(% His[d])	
	Cu[a]	s	p	d	S	Cys[b]	S	Met[b]	N[c]	His[b]
1	0.0	−0.1	0.4	−0.3	−1.0	0.1	0.3	0.0	0.2	0.0
2	0.6	−0.1	0.4	0.3	−2.8	−0.2	1.4	0.3	0.3	0.0
3	1.8	0.7	1.7	−0.6	−3.5	−0.3	0.6	0.1	0.2	0.1
2 + 3	3.5	0.8	1.5	1.2	−10.0	−1.1	5.8	0.7	0.4	0.0
NiR	3.8	0.7	1.7	1.4	−10.3	−1.2	5.8	0.8	0.4	0.0

[a] Total charge on the Cu ion. [b] Total charge for all atoms of the ligand except the S or N coordinated to Cu. [c] Total charge for coordinating N atoms. [d] Histidines are replaced by amines in these calculations.

shifted to higher energy by $\sim$1000 cm^{-1} compared to those in plastocyanin.

Through analysis of the spectroscopic features combined with density functional molecular orbital calculations presented here, the electronic structural origins of the perturbed spectral features in nitrite reductase are now well defined. The principal electronic structure changes responsible for the differences in the blue sites between nitrite reductase and plastocyanin are a rotation of the d$_{x^2-y^2}$ HOMO and an increased ligand field strength, which arise from a more tetragonal, flattened tetrahedral geometry, at the site in nitrite reductase relative to plastocyanin.

The rotation of the HOMO causes increased σ and decreased π overlap involving the cysteine and Cu d$_{x^2-y^2}$ orbitals. Therefore, as charge transfer transition intensities are proportional to the degree of overlap between the HOMO and ligand orbitals, the $\sim$450 nm band, which is assigned as the S(Cys) pseudo-σ → Cu 3d$_{x^2-y^2}$ transition, increases in intensity and the $\sim$600 nm blue band, assigned as S(Cys) pπ → Cu 3d$_{x^2-y^2}$, decreases in intensity. The rotation of d$_{x^2-y^2}$ also allows for significant mixing of S(Met) character into the HOMO in nitrite reductase which is not observed for plastocyanin. This mixing allows for additional charge transfer intensity in the nitrite reductase absorption spectrum involving the methionine ligand, and thus, the $\sim$385 nm band is assigned as the S(Met) b$_1$ → Cu 3d$_{x^2-y^2}$ transition. Additionally, this new S(Met)−Cu interaction in the HOMO accounts for the anomalously high S K-edge pre-edge intensity observed for nitrite reductase. The loss of sulfur covalency from the longer, weaker Cu−S(Cys) bond is offset by the increase in S(Met) covalency.

The increased ligand field strength caused by the geometric distortions at the site results in the shifting of the d → d transitions to higher energy. The shift in the ligand field transitions results in an increase in the nitrite reductase g values, which, in turn, account for the changes in $|A_z|$ for nitrite reductase relative to plastocyanin. Further, increased ligand field strength along the z-axis, resulting primarily from the shorter Cu−S(Met) distance in the site in nitrite reductase, will mix d$_{z^2}$ character into the HOMO which will cause rhombic splitting in the EPR spectrum. The degree of d$_{z^2}$ mixing into the HOMO in nitrite reductase determined here has been shown to be sufficient to explain the rhombic EPR spectrum of the site.

The rotation of d$_{x^2-y^2}$ and the increased ligand field strength at the site are caused by several geometric distortions. A minor role is played by an initial distortion of the site toward a more tetrahedral structure relative to plastocyanin, with a shorter Cu−S(Met) bond, longer Cu−S(Cys) bond, and greater displacement of the Cu ion out of the NNS plane toward S(Met). The dominant geometric factors responsible for the perturbed features in nitrite reductase involve coupled angular changes in the positions of the cysteine and methionine ligands. The overall effect of these distortions is that nitrite reductase adopts a more tetragonal structure compared with plastocyanin. The tetragonal distortion present in nitrite reductase involves a flattening of the pseudotetrahedral structure toward square planar.

In plastocyanin, the blue copper site geometry is a distorted tetrahedron. Tetrahedral Cu(II) complexes are found to tetragonally distort (most commonly a flattening of the tetrahedron toward square planar) due to the Jahn−Teller effect. However, for plastocyanin, the weak axial ligand field resulting from the long Cu−S(Met) bond imposed by the protein and the associated short Cu−S(Cys) bond lower the site symmetry to C_s.[55] These geometric features eliminate the electronic degeneracy of the ground state by splitting the d$_{x^2-y^2}$ and d$_{xy}$ orbitals by >10 000 cm^{-1}.[41] In tetrahedral complexes, these orbitals are much closer in energy, and it is this near degeneracy of these orbitals that would cause these complexes to undergo a Jahn−Teller distortion to a more tetragonal geometry. In nitrite reductase, the shorter Cu−S(Met) distance (2.55 Å versus 2.82 Å in plastocyanin) results in increased charge donation from the methionine, and thus, the cysteine bond lengthens[24] (2.17 Å versus 2.07 Å in plastocyanin[25]). If these bond lengths are introduced in the C_s distorted C_{3v} plastocyanin structure, the resulting more tetrahedral geometry would be expected to decrease the energy splitting between the d$_{x^2-y^2}$ and d$_{xy}$ orbitals. In fact, electronic structure calculations on a theoretical construct with these geometric changes relative to the plastocyanin structure (structure 1, Figure 6) indicate that the splitting of the d$_{x^2-y^2}$ and d$_{xy}$ orbitals will decrease by $\sim$2000 cm^{-1}. Therefore, the site in structure 1 is subject to an increased Jahn−Teller distorting force. This distorting force is defined by the value of the electronic-vibrational linear coupling term ($\delta V/\delta Q_i$, where V is the potential energy and Q_i is the normal mode of vibration),[91] evaluated over the ground state in structure 1. While the distortions involving the angular changes of the cysteine and methionine ligands in nitrite reductase have been treated separately thus far, they are in fact coupled, and as illustrated in Figure 7B, the combined distortion approximately corresponds to the $Q_i = \epsilon(u)$ tetrahedral normal mode of vibration which is a Jahn−Teller coordinate (Figure 7A).[92] Following the methodology in ref 55 used to determine the linear coupling terms for the normal modes in plastocyanin, the force along this distortion (which can be considered a reduction in the dihedral angle between the S(Met)−Cu−S(Cys) and N(His)−Cu−N(His) planes) can be calculated. It is found to be an order of magnitude greater in model 1 (0.046 eV/deg) than in plastocyanin (0.002 eV/deg). The force constants for the bending modes determined through a normal coordinate analysis on plastocyanin[55] range from 0.05 to 0.14 mdyn/Å. Calculating the expected magnitude of the tetragonal distortion using this range of force constants indicates that a complex with model 1's geometry can be expected to distort in the $\sim\epsilon(u)$ direction, as observed experimentally, by an angle of 10−25°. The calculated magnitude of this distortion compares favorably with the observed angular difference along this distortion between model 1 and nitrite reductase (20.6°).[24]

The electronic and geometric differences between nitrite reductase and plastocyanin can contribute to differences in the

(91) Solomon, E. I. *Comments Inorg. Chem.* **1984**, *3*, 225−320.
(92) Sturge, M. D. *Solid State Phys.* **1967**, *20*, 91−211.
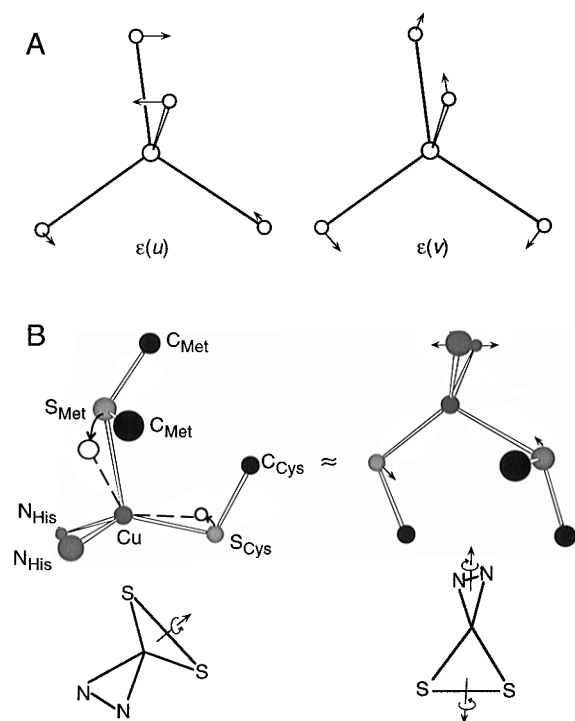
Figure 7. (A) Components of the e vibrational mode for a tetrahedral complex. (B) Correlation of the tetragonal distortions toward square planar responsible for the changes in the electronic structure of nitrite reductase relative to plastocyanin with the $\epsilon(u)$ tetrahedral vibrational mode. The distortions are represented by the rotations of the cysteine and methionine residues (left) (positions in nitrite reductase indicated by dashed ball and sticks) which can also be viewed as the movement of all residues (right). Stick figures (bottom) represent the same distortions in terms of the relative orientation of the S(Met)−Cu−S(Cys) and N(His)−Cu−N(His) planes.

reactivity of the sites. The distortion lowers the energy of the oxidized site which should lower its reduction potential (plastocyanin[93−95] $E° = 370$ mV, nitrite reductase[87] $E° = 240$ mV). Further, for the same driving force, the rate of electron transfer through the thiolate to a remote site should be affected by both the significantly reduced covalency of the Cu−S(Cys) bond (38% in plastocyanin versus ∼28% in nitrite reductase) and the mixed σ/π superexchange pathways due to the rotation of the $d_{x^2-y^2}$ HOMO. Finally, dependent on ligand−ligand interaction effects on the reduced site, there could be a larger Franck−Condon barrier to electron transfer.[25,93] Assessment of these possible contributions to differences in reactivity require further study of the reduced site in nitrite reductase and evaluation of its specific electron transfer pathways.

The tetragonally distorted oxidized site in nitrite reductase indicates that a greater Jahn−Teller distortion occurs at this site compared with the classic site in plastocyanin. As the entatic/rack state in blue copper proteins can be thought of as the protein environment preventing the Cu(II) site from undergoing a Jahn−Teller distortion toward a tetragonal site, the type 1 site in nitrite

reductase is in a "less entatic" (or reduced rack) state[48−51] than in plastocyanin. The origin of the reduction in the entatic nature of the site in nitrite reductase appears to correlate with the length of the Cu−S(Met) bond (or, more accurately, with the strength of the axial ligand field strength), which has been shown to be the principal geometric feature in plastocyanin attributable to an entatic/rack state. As the axial ligand field strength is increased with the shorter Cu−S(Met) bond, the charge donation to the Cu increases, the Cu is pulled farther out of the NNS plane, and the Cu−S(Cys) bond lengthens correspondingly. This would initially produce a more tetrahedral geometry, causing a reduction in the splitting of the $d_{x^2-y^2}$ and d_{xy} orbitals. With the reduction in the splitting of these orbitals, the site becomes subject to a tetragonal Jahn−Teller distortion, involving a coupled rotation of the cysteine and methionine residues, which further distorts the site toward a more square planar structure.

Finally, nitrite reductase appears to represent the limit along a continuum of perturbed blue copper sites, which spans the range from the very intense ∼600 nm, very weak ∼450 nm absorption bands in classic sites to the very intense ∼400 nm, very weak ∼600 nm bands in normal sites. Further tetragonal distortion in nitrite reductase should lead to a fairly normal Cu-(II) site with a thiolate ligand. Moderately perturbed sites such as pseudoazurin (Cu−S(Met) = 2.69 Å)[96] and cucumber basic blue protein (Cu−S(Met) = 2.62 Å)[97] which have stronger axial ligand fields and weaker Cu−S(Cys) interactions[17] than classic sites represent lesser degrees of the distortions present in nitrite reductase (Cu−S(Met) = 2.55 Å). Thus, they exhibit more tetrahedral structures and perturbed spectral features relative to the classic sites in plastocyanin (Cu−S(Met) = 2.82 Å)[25] and azurin (Cu−S(Met) = 3.13 Å)[27] without manifesting the extreme features in nitrite reductase.

(93) Sykes, A. G. *Adv. Inorg. Chem.* **1991**, *36*, 377−408.
(94) Büchi, F. N.; Bond, A. M.; Codd, R.; Huq, L. N.; Freeman, H. C. *Inorg. Chem.* **1992**, *31*, 5007−5014.
(95) Armstrong, F. A.; Hill, H. A. O.; Oliver, N.; Whitford, D. *J. Am. Chem. Soc.* **1985**, *107*, 1473−1476.

(96) Adman, E. T.; Turley, S.; Bramson, R.; Petratos, K.; Banner, D.; Tsernoglou, D.; Beppu, T.; Watanabe, H. *J. Biol. Chem.* **1989**, *264*, 87−99.
(97) Guss, J. M.; Merritt, E. A.; Phizackerlay, R. P.; Hedman, B.; Murata, M.; Hodgson, K. O.; Freeman, H. C. *Science* **1988**, *241*, 806−811.